

Review

Sustainable Biorefineries Based on Catalytic Biomass Conversion: A Review

Juan Camilo Solarte-Toro , Mariana Ortiz-Sanchez , Pablo-José Inocencio-García and Carlos Ariel Cardona Alzate *

Instituto de Biotecnología y Agroindustria, Departamento de Ingeniería Química, Universidad Nacional de Colombia sede Manizales, Manizales 170003, Colombia; jcsolartet@unal.edu.co (J.C.S.-T.); pinocencio@unal.edu.co (P.-J.I.-G.)

* Correspondence: ccardonaal@unal.edu.co

Abstract: Biorefineries have been profiled as potential alternatives to increase biomass use at the industrial level. However, more efforts are required to improve the sustainability of these facilities through process improvement and product portfolio increase. The catalytic conversion of biomass to chemicals and energy vectors is one of the most studied research lines today. The open literature has described catalytic pathways for producing biofuels and platform molecules using this renewable resource. Nevertheless, few literature reviews have aimed to analyze the role of the catalytic conversion of biomass in biorefineries while considering the following items: (i) biocatalysis, (ii) carbon dioxide conversion, (iii) design based on catalytic biomass upgrading, and (iv) sustainability metrics. This paper reviews several processes where catalysis has been applied to improve yields and conversion to elucidate the potential of this research field to boost biomass implementation in different productive sectors. This paper provides an overview of the catalytic conversion of biomass into a series of biofuels and high-value-added products, involving key topics related to catalyst performance, use, applications, and recent trends. In addition, several research gaps and ideas are highlighted based on previous studies. In conclusion, the catalytic conversion of biomass has the potential to increase biorefineries' sustainability. Nevertheless, more studies focused on (i) the production of new catalysts using renewable resources, (ii) the techno-economic and environmental assessment of processes involving catalysis, and (iii) the influence of involving biomass valorization via heterogeneous catalysis in existing facilities are required to obtain a real understanding of catalytic upgrades' benefits.

Keywords: biocatalysis; catalysts recycling and re-use; sustainability; process design; biofuels; platform molecules



Citation: Solarte-Toro, J.C.; Ortiz-Sanchez, M.; Inocencio-García, P.-J.; Cardona Alzate, C.A. Sustainable Biorefineries Based on Catalytic Biomass Conversion: A Review. *Catalysts* **2023**, *13*, 902. <https://doi.org/10.3390/catal13050902>

Academic Editors: Junaid Ahmad, Chawalit Ngamcharussrivichai, Rayya Ahmed Al-Balushi, Umer Rashid and Diego Luna

Received: 11 April 2023

Revised: 3 May 2023

Accepted: 9 May 2023

Published: 17 May 2023



Copyright: © 2023 by the authors. Licensee MDPI, Basel, Switzerland. This article is an open access article distributed under the terms and conditions of the Creative Commons Attribution (CC BY) license (<https://creativecommons.org/licenses/by/4.0/>).

1. Introduction

Energy matrix diversification has been categorized as the most reliable approach to guarantee energy security in different world regions [1]. Currently, most countries depend highly on non-renewable energy sources (i.e., crude oil, natural gas, coal). Price fluctuations and geopolitical conflicts can affect the power, electricity, building, industry, agriculture, and transport sectors [2]. This dependence is not convenient because any change in the global context can affect the economic and environmental goals proposed and discussed by international organizations (e.g., the UN). For instance, the Russian Federation's invasion of Ukraine has affected the energy transition goals and discourse of different European countries (e.g., Germany) [3]. Fossil fuel prices, especially coal, increased for heating and power generation in late 2021 [4]. This increased demand caused a domino effect in coal-exporting countries (e.g., Colombia), because the increase in coal prices reduced the profit margin of coal-dependent industries (e.g., brick-making industries). Therefore, energy matrix diversification is mandatory to guarantee a reliable, affordable, and efficient service for the world population.

Bioenergy has become one of the most important pillars in energy transition topics, as biomass can reduce greenhouse gas emissions (GHG) and environmental damages caused by the excessive use of fossil fuels [5]. Biomass is an alternative for energy production, as this renewable resource can contribute to accomplishing the requirements of the transport sector, especially in the aviation and marine sectors [4,6]. On the other hand, sustainable production and consumption patterns have awakened consumers' interest in bio-based products instead of synthetic ones. Therefore, biomass has been studied as a potential feedstock for producing biomaterials (e.g., bioplastics, biocomposites), bulk chemicals (organic acids, alcohols), nutraceutical products (e.g., antioxidants), biosurfactants (e.g., rhamnolipids, surfactin), and food additives (e.g., sweeteners and preservatives) [7,8].

Second-generation biomass has been profiled as a potential raw material to replace crude oil, as different research efforts have demonstrated the possibility of obtaining the same products with a lower environmental impact (e.g., olefins, paraffin) while avoiding food security issues [9]. Most studies involve lignocellulosic biomass fractionation and upgrading by implementing biotechnological, thermochemical, physical, and chemical processes [10]. Several reactions with specific activation energies and reaction pathways can occur when disrupting biomass, providing a complex mixture of degradation products as described for the evolution pathways of herbal tea waste when implementing hydrothermal conversion [11] (see Figure 1). Moreover, different process configurations have been proposed for the integral use of all lignocellulosic biomass fractions [12]. Nevertheless, the range of products derived from these processes is restricted, as more complex molecules require specific reaction conditions (i.e., temperature, pressure). Therefore, catalysis plays a key role in biomass conversion, as “new products” with a high yield, selectivity, and conversion are achieved at milder operating conditions [13].

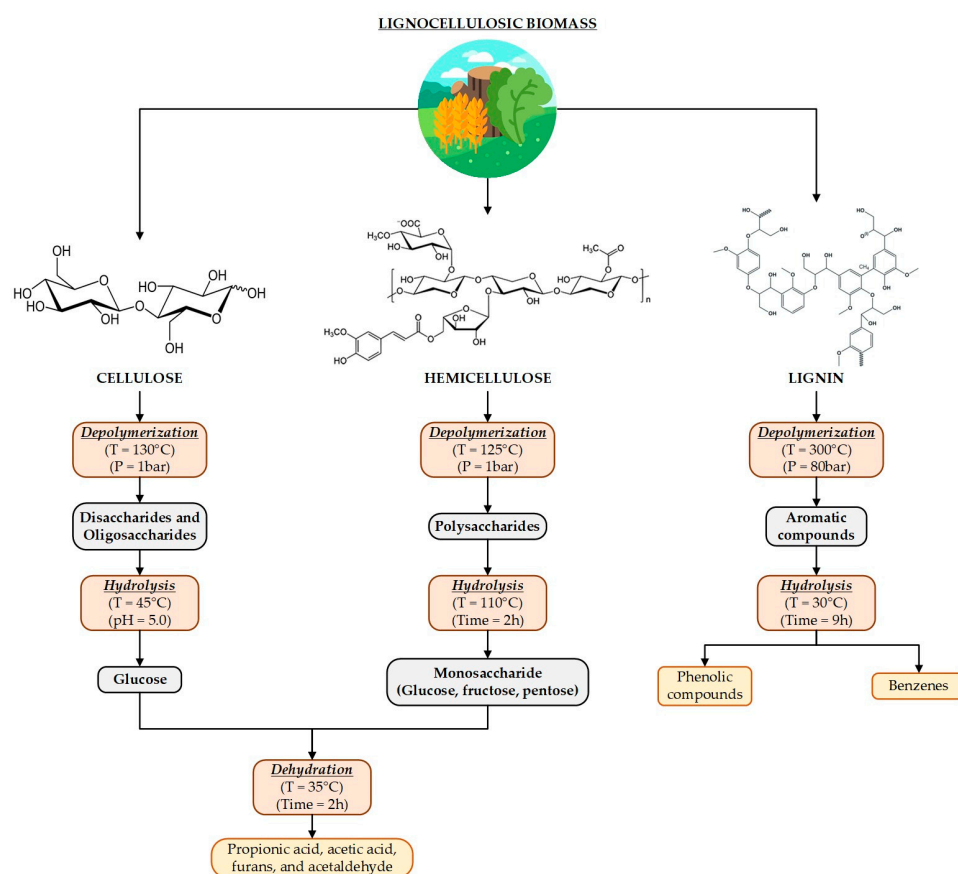


Figure 1. Reaction pathways for biomass components of herbal tea waste through hydrothermal conversion.

Catalysis occurs in almost all biomass-processing stages (i.e., pretreatment and conversion) [2]. Recent trends have promoted heterogeneous catalysis, considering possible catalyst recovery and re-use. Instead, homogenous catalysis has also been studied for most lignocellulosic biomass-upgrading processes (e.g., acid hydrolysis) [14]. Biomass-to-biofuels conversion through catalytic processes has been one of the most studied issues due to the low global implementation of bioenergy in the industrial and transport sectors for heat and power requirements [15]. In addition, high-value-added compounds produced via heterogeneous catalysis have been studied for the cosmetic, pharmaceutical, and chemical sectors. Thus, the integral processing of lignocellulosic biomass by implementing catalytic processes can help reach the proposed decarbonization and climate change mitigation goals. Furthermore, lignocellulosic biomass upgrading through catalytic processes avoids a structural and technological shift in the industry and transport sectors [16]. Advantages related to the catalytic upgrading of biomass are (i) improvement of different processes' sustainability by reducing energy requirements, (ii) production of platform molecules as a strong option to diversify the list of bio-based products derived from biomass, and (iii) reduction in waste streams [17]. Thus, lignocellulosic biomass conversion involving catalytic processes can contribute to reaching energy transition and fossil fuel independence goals faster.

Several reviews are devoted to describing catalytic pathways for biomass upgrading. Nevertheless, few literature reviews have aimed to analyze the catalytic upgrading of biomass while considering the following items: (i) biocatalysis' role in the production of specialty and fine chemicals, (ii) carbon dioxide conversion, (iii) biorefinery design based on catalytic biomass conversion, and (iv) sustainability metrics of biomass-upgrading processes involving homogeneous and heterogeneous catalysis. The novelty of this paper lies in highlighting the role of catalysis in boosting biomass use at the industrial level. Therefore, this paper provides an overview of the catalytic upgrading of biomass into a series of biofuels and high-value-added products, involving key topics related to catalysts' performance, use, applications, and recent trends. Furthermore, a comparison of technical, economic, and environmental metrics of different biomass-upgrading processes is presented to elucidate the influence of involving catalytic processes on biorefineries' sustainability.

2. Biorefineries and Catalytic Biomass Upgrading

Lignocellulosic biomass conversion in biorefineries has been analyzed based on the main biomass constituents. These facilities are complex systems where biomass is integrally processed or fractionated to obtain more than one product, including bioenergy, biofuels, chemicals, and high-value-added compounds [18]. Biorefineries are designed while considering a comprehensive study of the raw materials and promising technologies [19]. These facilities have been proposed as the starting point for developing and implementing a consolidated bioeconomy [20]. Thus, biorefineries can help to accomplish the Sustainable Development Goals (SDGs) proposed by the UN.

Biorefineries' implementation has been slowed, as current technologies upgrade non-renewable resources at the industrial level. Therefore, the transition from crude-oil refineries to biorefineries remains slow compared to the research on biomass upgrading at a lab scale [21]. A path towards easier industrial biomass use, leaving aside traditional uses (i.e., combustion), is to upgrade biomass-derived products through catalytic processes to obtain chemicals without requiring an in-depth technological transition. Therefore, catalysis is crucial for (i) shortening distances between academia and industry regarding biomass use, (ii) enhancing biorefinery designs, (iii) creating new biomass conversion pathways, and (iv) increasing processes' sustainability. Biorefineries comprise thermochemical, biotechnological, chemical, and physical processes through which several compounds can be produced. Thus, catalytic upgrading can be present in all these processes. Indeed, several research efforts have demonstrated the importance of applying catalysis to improve technical indicators (i.e., yields, productivity, and product purity) [22]. These improvements

are discussed while considering thermochemical biomass upgrading and catalytic biomass fractionation as follows.

2.1. Thermochemical Biomass Upgrading

2.1.1. Pyrolysis

Pyrolysis produces biochar, bio-oil, gases (e.g., hydrogen, methane), and other minor by-products such as acetone, methanol, phenol, acetic acid, and BTX. This process is performed under anoxic conditions (i.e., a total absence of oxygen and any other oxidizing agent). Thus, pyrolysis operates with an equivalence ratio (ER) equal to zero. This process occurs between 300 °C and 600 °C [23]. Pyrolysis can be classified as fast, intermediate, or slow according to the operating conditions, especially the heating rate and the feedstock residence time. Solarte-Toro et al. [24] described the most important characteristics of these processes and the different reactor types used at the industrial level. In synthesis, fast pyrolysis is directed to produce bio-oil, while slow pyrolysis is driven to produce biochar.

Catalytic pyrolysis processes reported in the open literature aim to improve yields and bio-oil composition (see Table 1). Depending on the location of the catalyst, the catalytic pyrolysis can be classified as an in situ or ex situ process. In situ pyrolysis is applied when biomass is mixed with the catalyst and processed together in the reactor. In contrast, ex situ pyrolysis upgrades the outlet stream from the process by increasing the main products content [25]. Bio-oil yields vary depending on the biomass source (e.g., agro-industrial wastes can produce more bio-oil than forestry biomass). Nevertheless, bio-oil has a high oxygen content regardless of the biomass source. Thus, a fast-pyrolysis product has a lower heating value than conventional fossil fuels [26]. Catalysts were included to improve bio-oil quality in terms of heating value, water content, oxygen content, acidity, viscosity, and chemical composition in fast pyrolysis processes, as the bio-oil composition is affected by the raw material C, H, O, N, and S contents (i.e., higher O/C ratios affect bio-oil quality). Indeed, catalytic fast pyrolysis reduces the oxygenated compounds through catalytic reactions, such as cracking, deoxygenation, decarboxylation, decarbonylation, hydrodeoxygenation, and hydrogenation [27].

Catalysts applied in fast pyrolysis processes are zeolites, mesoporous silica oxides, metal compounds, metal oxides, red mud, and bentonite (see Table 1). Zeolites (acid catalyst) cause cellulose decomposition into anhydro-sugars via dehydration reactions. These products are upgraded to low-molecular-weight olefins (C₂–C₆). Then, short hydrocarbons are combined to produce aromatic compounds. Instead, hemicellulose and lignin suffer depolymerization, dehydration, and decarbonylation reactions to produce aromatic compounds and olefins, as described by Rahman et al. [28]. Moreover, as described by Dada et al. [29], the corresponding catalyst molecules (e.g., Metal/ZSM-5) can potentially be used to produce high-quality bio-oil in terms of thermal stability and low viscosity and corrosiveness, which are properties that cannot be achieved through conventional pyrolysis processes.

Table 1. Catalytic pyrolysis of lignocellulosic biomass: yields and catalyst effect.

Feedstock	VM/FC *	Catalyst	Operating Conditions	Reactor	Pyrolysis	Yield (wt%)			Catalyst Effect	Ref.
						Bio-Oil ^a	Biochar	Gases		
Poplar sawdust	4.76	ZSM-5 zeolite (Si/Al = 25)	T: 550 °C; O.T. 60 min; Load: 20 g biomass and 20 g catalyst; in situ catalysis; C.G.: N ₂ ; N ₂ flow rate: 100 mL/min.	Fixed-bed reactor	Fast pyrolysis	28.63	30.63	40.75	N.R.	[30]
Pine sawdust	5.79	HZSM-5	T: 400 °C; O.T.: 30 min; Load: 25 g biomass and 6.25 g catalyst; B.P.S.: <1.18 mm; in situ catalysis; C.G.: N ₂ ; N ₂ flow rate: 100 mL/min.	Fixed-bed reactor	Fast pyrolysis	36.60	34.28	29.12	Bio-oil and gases yields decrease, and biogas yield increases.	[31]
Pine sawdust	5.79	Ni/HZSM-5	T: 400 °C; O.T.: 30 min; Load: 25 g biomass and 6.25 g catalyst; B.P.S.: <1.18 mm; in situ catalysis; C.G.: N ₂ ; N ₂ flow rate: 100 mL/min.	Fixed-bed reactor	Fast pyrolysis	35.34	37.94	26.72	Bio-oil and gases yields decrease, and biogas yield increases.	[31]
Cellulose from switchgrass	5.34	ZSM5 (CBV2314 with SiO ₂ /Al ₂ O ₃ ratio of 23)	T: 600 °C; C/B: 20; C.G.: He ₂ ; He ₂ flow rate: 1 mL/min; in situ catalysis.	Micro-furnace pyrolyzer	Fast pyrolysis	35.29	33.22	31.49	N.R.	[32,33]
Chips of pine	6.58	CoMo-S/Al ₂ O ₃	T: 863 K; O.T.: 40 min; H.R.: 32 K/min; Biomass diameter: 104 µm; in situ catalysis.	Powder-particle fluidized bed (PPFB)	Slow pyrolysis	11.49	44.48	44.04	N.R.	[34]
Chips of Alaskan spruce	7.01	CoMo-S/Al ₂ O ₃	T: 863 K; O.T.: 40 min; H.R.: 32 K/min; Biomass diameter: 104 µm; in situ catalysis.	Powder-particle fluidized bed (PPFB)	Slow pyrolysis	6.06	47.63	46.31	N.R.	[34]
Chips of tropical lauan	6.55	CoMo-S/Al ₂ O ₃	T: 863 K; O.T.: 40 min; H.R.: 32K/min; Biomass diameter: 104 µm; in situ catalysis.	Powder-particle fluidized bed (PPFB)	Slow pyrolysis	6.27	44.11	49.62	N.R.	[34]
Mixture of pine and spruce	5.00	VS ₂ (Vanadia content: 2.5 wt%)	T: 450 °C; O.T.: 90 min; in situ catalysis; B.P.S.: 1.0–1.4 mm; Biomass feeding ratio: 2 kg/h; Support material: SiO ₂ .	Bubbling fluidized-bed reactor	Fast pyrolysis	61.14	38.86	N.R.	Bio-oil yield decreases, and char yield remains the same.	[35,36]
Commercial lignocellulosic biomass (Lignocel HBS 150–500) from beech wood	3.64	ZSM-5/A (zeolite formulation diluted with silica–alumina)	T: 500 °C; O.T.: 25 min; R.T.: 0.03 s; in situ catalysis; Load: 1.5 g biomass and 0.7 g catalyst; C.G.: N ₂ .	Circulating-fluid-bed reactor	Fast pyrolysis	27.35	35.93	36.72	Bio-oil yield decreases, and biochar and gases yields increase.	[37,38]
	3.64	ZSM-5/B catalyst)	T: 500 °C; O.T.: 25 min; R.T.: 0.03 s; in situ catalysis; Load: 1.5 g biomass and 0.7 g catalyst; C.G.: N ₂ .	Circulating-fluid-bed reactor	Fast pyrolysis	32.65	34.68	32.67	Bio-oil yield decreases, and biochar and gases yields increase.	[37,38]
	3.64	Co/ZSM-5/A (zeolite promoted with 5 wt% Co)	T: 500 °C; O.T.: 25 min; R.T.: 0.03 s; in situ catalysis; Load: 1.5 g biomass and 0.7 g catalyst; C.G.: N ₂ .	Circulating-fluid-bed reactor	Fast pyrolysis	22.49	35.48	42.03	Bio-oil yield decreases, and biochar and gases yields increase.	[37,38]
	3.64	Co/ZSM-5/B (catalyst promoted with 5 wt% Co)	T: 500 °C; O.T.: 25 min; R.T.: 0.03 s; in situ catalysis; Load: 1.5 g biomass and 0.7 g catalyst; C.G.: N ₂ .	Circulating-fluid-bed reactor	Fast pyrolysis	23.21	34.95	41.84	Bio-oil yield decreases, and biochar and gases yields increase.	[37,38]

Table 1. Cont.

Feedstock	VM/FC *	Catalyst	Operating Conditions	Reactor	Pyrolysis	Yield (wt%)			Catalyst Effect	Ref.
						Bio-Oil ^a	Biochar	Gases		
White oak wood	4.67	Ca/Y zeolite	T: 500 °C; B.P.S.: 2 mm; Load: 260 g biomass and 800 g catalyst; in situ catalysis; C.G.: N ₂ ; N ₂ flow rate: 85 L/min.	Bubbling fluidized-bed reactor	Fast pyrolysis	42.86	18.57	38.57	Bio-oil and biochar yields decrease, and gases yield increases.	[39,40]
Coal and cedar wood	2.33	USY zeolite (metal-modified ultra-stable Y type)	T: 600 °C; O.T.: 2 h; in situ catalysis; C.G.: Ar; Ar flow rate: 100 mL/min.	Dropdown tube reactor	Fast pyrolysis	44.94	45.38	9.68	N.R.	[41,42]
Rice husk	5.00	4% Fe/ZSM-5	T: 550 °C; O.T.: 30 min; Load: 3 g biomass and 15 g catalyst; in situ catalysis; C.G.: N ₂ ; N ₂ flow rate: 200 mL/min.	Two-stage fixed-bed reactor	Fast pyrolysis	29.44	34.28	36.28	Bio-oil yield decreases, and gases yield increases.	[43]
Sugarcane bagasse	3.83	HZSM-5 (Si/Al = 23 in protonic form)	T: 500 °C; B.P.S.: 0.5 mm; C/B: 0.5/1.0; in situ catalysis; C.G.: N ₂ ; N ₂ flow rate: 50 mL/min.	Fixed-bed reactor	Fast pyrolysis	52.98	28.10	18.92	Bio-oil and gases yields decrease, and biochar yield increases.	[44]
Wheat straw	1.80	H-ZSM-5 (Si/Al ratio = 30:4)	T: 350 °C; O.T.: 1 h; C/B: 0.1/1.0; B.P.S.: 0.5–1.0 mm; Solid phase contact; H.R.: 25 °C/min; in situ catalysis; C.G.: N ₂ ; N ₂ flow rate: 50 mL/min.	Fixed-bed reactor	Slow pyrolysis	27.90	37.10	35.00	Bio-oil and gases yields decrease, and biochar yield increases.	[45,46]
Wheat husk	1.71	H-ZSM-5 (Si/Al ratio = 30:4)	T: 350 °C; O.T.: 1 h; C/B: 0.1/1.0; B.P.S.: 0.5–1.0 mm; Solid phase contact; H.R.: 25 °C/min; in situ catalysis; C.G.: N ₂ ; N ₂ flow rate: 50 mL/min.	Fixed-bed reactor	Slow pyrolysis	19.00	31.40	49.60	Bio-oil and biochar yields decrease, and gases yield increases.	[46,47]
<i>C. limon</i> peel	5.23	Al-MCM-41 (SiO ₂ /Al ₂ O ₃ = 40)	T: 500 °C for biomass reactor and 600 °C for catalytic reactor; H.R.: 7 °C/min; Load: 2 mg powder biomass, 10 mg catalyst; ex situ catalysis; C.G.: N ₂ .	Tandem micro-reactor-GC/MS	Slow pyrolysis	17.53	37.11	45.36	N.R.	[48]
<i>Citrus paradisi</i> peel	6.18	Al-MCM-41 (SiO ₂ /Al ₂ O ₃ = 40)	T: 500 °C for biomass reactor and 600 °C for catalytic reactor; H.R.: 7 °C/min; Load: 2 mg powder biomass, 10 mg catalyst; ex situ catalysis; C.G.: N ₂ .	Tandem micro-reactor-GC/MS	Slow pyrolysis	18.56	32.99	48.45	N.R.	[48]
Switchgrass	1.61	Bentonite (Al ₂ O ₃ SiO ₂ H ₂ O)	T: 400 °C; H.R.: 20 °C/min; B.P.S.: 0.125 mm; C.P.S.: <0.050 mm; Biomass concentration: 30 wt%; Microwave power: 750 W.	Microwave-assisted reactor	Fast pyrolysis	38.78	27.55	33.67	Bio-oil, biochar, and gases yields increase.	[49,50]

* VM/FC: Volatile matter to fixed carbon ratio. ^a: Organic fraction + Aqueous fraction. T: Temperature. O.P.: Operating time. H.R.: Heating rate. R.T.: Residence time. B.P.S.: Biomass particle size. C.P.S.: Catalyst particle size. C/B: Catalyst-to-biomass ratio. N.R.: None reported.

Bio-oil yields through catalytic pyrolysis of lignocellulosic biomass are similar to those reported without catalysts. There are different reports where the bio-yield decreases (see Table 1). Chen et al. [51] have reported smaller bio-oil yields with higher deoxygenation grade. For instance, catalytic fast pyrolysis of lignocel HBS 150–500 (beechwood sawdust with particle size 150–500 μm) changed according to the catalyst used [52]. H/C and O/C ratios decrease to 40% and 90% when using heterogeneous catalysis. Then, high heating values are achieved. The influence of using catalysts in fast pyrolysis on bio-oil properties is presented in Table 2. After catalytic pyrolysis, the H/C and O/C ratios are lower than the original biomass (see Table 2). On the other hand, the gas composition varies depending on the solid catalyst type. Pyrolysis gases comprise CO_2 , H_2 , CH_4 , CO , and light hydrocarbons. Calcium and aluminum oxides decrease the CO_2 content due to the adsorption of this compound while increasing the H_2 content. In contrast, transition metal oxides (e.g., TiO_2 , ZrO_2 , ZnO , and NiO) increase CO_2 content [51].

Several kinetic methods have been proposed to describe the chemical species behavior in the fast pyrolysis processes. For instance, the kinetic model proposed by Humbird et al. [53] provides a good approximation for the bio-oil, biochar, and gases obtained from different lignocellulosic biomass, as this model is based on the cellulose, hemicellulose, and lignin content. On the other hand, the pyrolysis process can be modeled using the ultimate analysis of biomass due to the several reactions involved in the thermal degradation process [54]. Nevertheless, the kinetic study and proper chemical compound production pathways are not completely clear. This issue is more evident for simulating the catalytic fast pyrolysis process, as tar-cracking reactions (among others) must be involved, and activation energies in the entire model must be estimated. In this sense, simulation procedures describing catalytic fast pyrolysis are uncommon in the open literature. Therefore, the kinetic study of catalytic fast pyrolysis is a research gap, as chemical species behavior understanding can help to elucidate optimal operating conditions according to the desired process outputs.

2.1.2. Gasification

Gasification is the partial oxidation of carbonaceous materials to obtain synthesis gas (syngas) composed of CO , H_2 , CH_4 , and CO_2 . Syngas has been used as an energy carrier (i.e., biofuel) and raw material for the catalytic production of methanol, dimethyl ether (DME), diesel-like fuel, and hydrogen [55]. Typical syngas after gasification has a mean composition of H_2 (15–20%), CO (15–20%), CH_4 (1–3%), CO_2 (8–12%), and N_2 (45–50%) [56]. Nevertheless, syngas composition varies depending on the type of raw material (e.g., coal, petcoke, and biomass) and the gasifying agent (i.e., O_2 , steam, CO_2 , and air) [57]. Different improvements of the gasification process have been developed and proposed to increase the H_2/CO ratio. In addition, reactor configuration and operating process parameters have been changed through innovative designs. Catalytic gasification, steam gasification, solar-thermal gasification, supercritical water gasification, microwave-assisted gasification, plasma gasification, multi-step gasification, and chemical-looping gasification are possible routes for increasing the H_2/CO ratio after lignocellulosic biomass gasification. This review paper addresses catalytic gasification, but the other gasification options have been reviewed by Ghodke et al. [58].

Table 2. Effect of the catalytic pyrolysis on the H/C and O/C atomic ratios of different lignocellulosic biomass.

Raw Material	Catalyst	Operating Conditions	Bio-Oil ^a Yield (wt%)	Elemental Composition (wt%)				Atomic Ratios		HHV (MJ/kg)	Ref.
				C	H	O	N	H/C	O/C		
Forest pine woodchips (<i>Pinus halepensis</i>)	No catalyst	T: 450 °C; C/B: 1/6; B.P.S.: 15 mm; A.R.C.: 100 kW of woody biomass.	49.20	60.60	7.70	31.50	0.20	0.13	0.52	26.38	[59]
	Bentonite	T: 450 °C; C/B: 1/6; B.P.S.: 15 mm; C.P.S.: 0.300 mm; A.R.C.: 100 kW of woody biomass; in situ catalysis.	46.28	62.66	7.61	29.53	0.20	0.12	0.47	27.24	[59]
	Sepiolite	T: 450 °C; C/B: 1/6; B.P.S.: 15 mm; C.P.S.: 0.300 mm; A.R.C.: 100 kW of woody biomass; in situ catalysis.	46.28	61.90	7.60	30.30	0.20	0.12	0.49	26.86	[59]
	Attapulgit	T: 450 °C; C/B: 1/6; B.P.S.: 15 mm; C.P.S.: 0.300 mm; A.R.C.: 100 kW of woody biomass; in situ catalysis.	45.00	63.40	7.80	28.60	0.20	0.12	0.45	27.91	[59]
	Red mud	T: 450 °C; C/B: 1/6; B.P.S.: 15 mm; C.P.S.: 0.300 mm; A.R.C.: 100 kW of woody biomass; in situ catalysis.	49.20	62.56	7.51	29.63	0.30	0.12	0.47	27.04	[59]
<i>Eremurus spectabilis</i>	No catalyst	T: 550 °C; H.R.: 50 °C/min; B.P.S.: 0.850 mm; Biomass load: 20 g; Fixed-bed tubular reactor; Sweeping gas flow: 100 mL/min.	33.50	58.96	6.77	32.81	1.46	1.38	0.42	23.79	[60]
	Tincal	T: 550 °C; H.R.: 50 °C/min; B.P.S.: 0.850 mm; Biomass load: 20 g; Fixed-bed tubular reactor; Sweeping gas flow: 100 mL/min; in situ catalysis.	37.25	57.73	6.98	34.07	1.22	1.45	0.44	23.45	[60]
	Colemanite	T: 550 °C; H.R.: 50 °C/min; B.P.S.: 0.850 mm; Biomass load: 20 g; Fixed-bed tubular reactor; Sweeping gas flow: 100 mL/min; in situ catalysis.	33.45	58.34	6.82	33.50	1.34	1.40	0.43	23.53	[60]
	Ulexite	T: 550 °C; H.R.: 50 °C/min; B.P.S.: 0.850 mm; Biomass load: 20 g; Fixed-bed tubular reactor; Sweeping gas flow: 100 mL/min; in situ catalysis.	34.00	59.71	6.93	31.99	1.37	1.39	0.40	24.42	[60]
Forest pine woodchips (<i>Pinus halepensis</i>)	No catalyst	T: 450 °C; R.T.: 2 h; C/B: 1/3; Biomass flow: 2 kg/h; A.R.C.: 100 kW of woody biomass; C.G.: N ₂ ; N ₂ flow rate: 5 L/min.	47.50	60.60	7.70	31.50	0.20	1.38	0.42	23.79	[61]
	CaO	T: 450 °C; R.T.: 2 h; C/B: 1/3; C.P.S.: 0.600 mm; Flows: 2 kg/h biomass and 6 kg/h catalyst; A.R.C.: 100 kW of woody biomass; C.G.: N ₂ ; N ₂ flow rate: 5 L/min; in situ catalysis.	48.72	67.90	7.60	24.20	0.30	0.11	0.36	29.79	[61]
Forest pine woodchips (<i>Pinus halepensis</i>)	CaO-MgO	T: 450 °C; R.T.: 2 h; C/B: 1/3; C.P.S.: 0.600 mm; Flows: 2 kg/h biomass and 6 kg/h catalyst; A.R.C.: 100 kW of woody biomass; C.G.: N ₂ ; N ₂ flow rate: 5 L/min; in situ catalysis.	48.94	66.80	7.50	25.40	0.30	0.11	0.38	29.10	[61]
Mediterranean sea plant (<i>Posidonia Oceanica</i>)	No catalyst	T: 500 °C; Atmospheric pressure; H.R.: 60 °C/min; R.T.: 1 h; Biomass load: 3 g; Biomass concentration: 25.66 wt%; C/B: 3/7; Stainless-steel fixed-bed reactor; C.G.: N ₂ ; N ₂ flow rate: 50 mL/min.	47.74	60.77	5.36	30.23	3.64	0.09	0.50	24.44	[62]
	CeO ₂	T: 500 °C; Atmospheric pressure; H.R.: 60 °C/min; R.T.: 1 h; Biomass load: 3 g; Biomass concentration: 25.66 wt%; C/B: 3/7; Stainless-steel fixed-bed reactor; C.G.: N ₂ ; N ₂ flow rate: 50 mL/min; in situ catalysis.	51.15	84.04	6.98	6.90	2.08	0.08	0.08	36.72	[62]
	NiCe/HZSM5	T: 500 °C; Atmospheric pressure; H.R.: 60 °C/min; R.T.: 1 h; Biomass load: 3 g; Biomass concentration: 25.66 wt%; C/B: 3/7; Stainless-steel fixed-bed reactor; C.G.: N ₂ ; N ₂ flow rate: 50 mL/min; in situ catalysis.	50.66	81.73	6.87	8.85	2.54	0.08	0.11	35.43	[62]

Table 2. Cont.

Raw Material	Catalyst	Operating Conditions	Bio-Oil ^a Yield (wt%)	Elemental Composition (wt%)				Atomic Ratios		HHV (MJ/kg)	Ref.
				C	H	O	N	H/C	O/C		
<i>A. azurea</i> plant stalks	No catalyst	T: 550 °C; H.R.: 100 °C/min; R.T.: 30 min; Biomass load: 20 g; C.G.: N ₂ ; N ₂ flow rate: 100 mL/min; Tubular fixed-bed reactor.	30.84	45.59	7.11	45.72	1.58	1.87	0.75	17.43	[63]
	Na ₂ CO ₃	T: 550 °C; H.R.: 100 °C/min; R.T.: 30 min; Biomass load: 20 g; C.G.: N ₂ ; N ₂ flow rate: 100 mL/min; Tubular fixed-bed reactor.	31.88	57.06	7.48	32.75	2.71	1.57	0.43	24.18	[63]
	Al ₂ O ₃	T: 550 °C; H.R.: 100 °C/min; R.T.: 30 min; Biomass load: 20 g; C.G.: N ₂ ; N ₂ flow rate: 100 mL/min; Tubular fixed-bed reactor.	32.10	49.90	7.43	41.23	1.44	1.78	0.62	20.16	[63]

^a: Organic fraction + Aqueous fraction. T: Temperature. C/B: Catalyst-to-biomass ratio. B.P.S.: Biomass particle size. C.P.S.: Catalyst particle size. A.R.C.: Auger Reactor Capacity. H.R.: Heating rate. R.T.: Reaction time. C.G.: Carrier gas. N.R.: None reported.

Syngas quality is determined by properties such as (i) heating value, (ii) H₂/CO ratio, and (iii) tar content. Then, these properties are optimized (or improved) by changing the operating conditions, promoting tar cracking, and crucial reactions (e.g., Boudouard and water–gas shift reactions) [64]. Catalytic gasification increases syngas quality by adding a catalyst into the process. In the same way as occurs with pyrolysis processes, gasification can be carried out through in situ and ex situ catalysis. Table 3 summarizes different syngas compositions and yields obtained after the catalytic gasification of lignocellulosic biomass reported in the open literature. In the same way as catalytic pyrolysis, there are several kinds of catalysts (i.e., metals, no metals, transition metals). Calcium oxide and dolomite are the most used catalysts in gasification processes (see Table 3). Other used catalysts are alkali, nickel, zirconia, and ruthenium-based catalyst [58].

Calcium oxide and dolomite are cheaper catalysts. Therefore, the use of these compounds increases the sustainability of the process, as the technical (more H₂), economic (lower expenses and higher incomes), and environmental (low tar production) performance of the gasification process is improved. Nevertheless, calcium oxide and dolomite are susceptible to poisoning and deactivation. Moreover, both catalysts (especially dolomite) are unstable at higher temperatures, which decreases possible industrial applications. Other catalysts are better than calcium oxide and dolomite, but higher operational expenditures are required [58]. Indeed, the ruthenium-based catalyst is a better catalyst than nickel, rhodium, and other transition metals. Even so, the catalyst cost makes its application at the industrial level unfeasible, if no high-value-added products are involved in the gasification plant.

Syngas quality (i.e., H₂ and CO content) increases when using a catalyst in the gasification process. After the increase in H₂ and CO content, syngas can be used to produce several products (e.g., methanol, and fuels). The Fischer–Tropsch process upgrades syngas to oil-like products (i.e., paraffin and olefins), which can be further converted into a wide range of liquid fuels (jet fuels, diesel, wax, naphtha). The H₂/CO ratio needed for the use of syngas in the Fischer–Tropsch process is between 1.8 and 2.1 using iron- or cobalt-based catalysts. Catalysis in biomass gasification plants plays a key role, as most of the H₂/CO ratios obtained in processes without catalysis are lower than 1.8 [65]. Indeed, if the air is used as gasifying agent, the ratios are lower than 1.0. Thus, the syngas use is limited. Methanol requires a high H₂/CO ratio between 5.0 and 8.0, and several kinetic studies have been developed for understanding this process [66]. Thus, catalysis helps to increase the application range of syngas.

Regarding the above context, a thermochemical plant based on biomass gasification requires catalysts for obtaining bulk products, fuel additives, and fuels. Thus, studies focused on optimizing catalysts or finding new catalysts are required, as this area (catalysis) is fundamental for guaranteeing a sustainable process over time. Some ideas reported in the open literature are related to the use of ashes as catalysts, as oxide metals such as SiO₂, Al₂O₃, Fe₂O₃, CaO, MgO, and SO₃ can be found. This composition provides alkali-based catalysis. Then, an increase in the H₂ content can be obtained (theoretically). However, slagging can be produced in the gasification reactor due to the high temperatures reached during the process (>700 °C). Zhang et al. [67] investigated the ash fusion characteristics and gasification reactivity of wheat straw (WS) blended with rice husk (RH) and wood dust (WD). These authors found that the maximum ratios of WS for WS/RH and WS/WD mixtures are 60% and 32% to avoid slagging, respectively. Moreover, the gasification process performance increases when using rice husk ashes. Therefore, the use of ashes can be a future research trend for improving the syngas quality using cheaper and renewable materials.

Table 3. Catalytic gasification of lignocellulosic biomass: yields and catalyst effect.

Raw Material	VM/FC *	Catalyst	Operating Conditions	Gasifier Type	Product Characterization		Catalyst Effect	Ref.
					Syngas Composition (v/v%)	H ₂ /CO		
Pine sawdust	4.38	Calcined dolomite-based	T: 800 °C for catalyst bed reactor; Flows: 0.47 kg/h biomass, 14 g/h catalyst, 0.65 Nm ³ /h air, and 0.40 kg/h steam; Load: 56 g catalyst; G.A.: air + steam; G.A./Biomass: 0.85; ex situ catalysis.	Fluidized-bed reactor	Dry, inert-free gas composition: H ₂ : 52.79, CH ₄ : 2.91, CO: 14.47, CO ₂ : 29.83	3.65	H ₂ content decreases while the other fractions' content increases.	[68]
Wood sawdust	4.09	Ca-added Ni-based catalyst	T: 550 °C for biomass reactor and 800 °C for catalyst bed reactor; H.R.: 40 °C/min; R.T.: 40 min; B.P.S.: <0.2 mm; Load: 1.0 g biomass and 0.5 g catalyst; Gas/wood (wt%): 74.4; G.A.: Steam. Water injection rate: 4.74 g/h, ex situ catalysis.	Fixed-bed two-stage reactor	Dry, inert-free gas composition: H ₂ : 49.20, CH ₄ : 7.73, CO: 22.49, CO ₂ : 20.58	2.19	H ₂ production increased when implementing catalysts.	[69]
	4.09	Ni/MCM-41 (40 wt% Ni)	T: 550 °C for biomass reactor and 800 °C for catalyst bed reactor; H.R.: 40 °C/min; R.T.: 40 min; Load: 0.80 g biomass and 0.25 g catalyst; B.P.S.: <0.2 mm; Gas/wood (wt%): 62.8; Residue/wood (wt%): 28.8; ex situ catalysis.	Fixed-bed two-stage reactor	Dry, inert-free, gas composition: H ₂ : 51.16, CH ₄ : 3.54, CO: 26.69, CO ₂ : 18.60	1.92	H ₂ production increased as well as that of CO ₂ . CO and CH ₄ content decrease.	[70]
Wet pig manure	7.72	Ni/Al ₂ O ₃ (20 wt% Ni, 0.5–1.2 mm)	T: 750 °C; H.R.: 10 °C/min; Load: 5.0 g biomass; C.G.: Ar; Ar flow rate: 120 mL/min; ex situ catalysis.	Two-stage fixed-bed quartz reactor	H ₂ : 60.66, CH ₄ : 4.92, CO: 21.31, CO ₂ : 13.11	2.85	All fractions' content increases with the catalyst.	[71,72]
Sewage-sludge-derived volatiles	7.66	Ni/LYLC (19 wt% Ni; 0.5–1.0 mm)	T: 900 °C for biomass reactor and 650 °C for catalysts bed reactor; H.R.: 10 °C/min; R.T.: 1.5 h; Load: 1.0 g SSDVs and 3.0 g catalyst	Two-stage fixed-bed reactor	H ₂ : 69.14, CH ₄ : 2.47 CO: 9.88, CO ₂ : 18.52	7.00	N.R.	[73]
Dehydrated corncob	4.45	Ni-exchanged resin char (Ni/RC) (18.0 wt% Ni)	T: 900 °C for biomass reactor and 650 °C for catalyst bed reactor; H.R.: 10 °C/min; Load: 1 g biomass. B.P.S.: 0.5–1.0 mm; C.G.: Ar. G.A.: Steam; ex situ catalysis.	Two-stage fixed-bed reactor	H ₂ : 53.66, CH ₄ : 4.88, CO: 36.59, CO ₂ : 4.88	1.47	All fractions' content increases with the catalyst.	[74,75]
Almond shells	1.55	Perovskite (LaNi _{0.3} Fe _{0.7} O ₃)	T: 770 °C; H.R.: 5 °C/min; Load: 280 g catalyst; B.P.S.: 1.1 mm; C.G.: N ₂ ; G.A.: Steam; G.A./Biomass: 0.3 kg/h; ex situ catalysis.	Two-stage fixed-bed quartz reactor (TSFBQR)	Dry, inert-free, gas composition: H ₂ : 58.80, CH ₄ : 3.10, CO: 25.90, CO ₂ : 12.20	2.27	H ₂ and CO fractions increase while CO ₂ and CH ₄ decreases	[76]
Sugarcane bagasse	5.94	Na ₂ CO ₃	T: 650 °C; H.R.: 10 °C/min; Biomass loading: 12 wt%; Catalyst loading: 20 wt%; G.A.: Steam. Steam flow rate: 20 mL/min; in situ catalysis.	Batch system reactor	H ₂ : 34.85, CH ₄ : 10.98, CO: 2.93, CO ₂ : 51.24	11.90	H ₂ production increased.	[77]
	5.94	Dolomite (CaMg(CO ₃) ₂) and sand (1:2 wt%)	T: 700 °C; Load: 1 kg biomass; B.P.S.: 2.5 cm; G.A.: Steam and air; G.A./Biomass: 0.5; in situ catalysis.	Fluidized-bed gasifier	H ₂ : 30.87, CH ₄ : 10.89 CO: 46.26, CO ₂ : 10.97	0.65	N.R.	[77,78]

Table 3. Cont.

Raw Material	VM/FC *	Catalyst	Operating Conditions	Gasifier Type	Product Characterization		Catalyst Effect	Ref.
					Syngas Composition (v/v%)	H ₂ /CO		
Rice husk	5.62	Uncalcined dolomite	T: 850 °C; H.R.: 15 °C/min; Biomass particle diameter: 1.5 mm; Feeding rate: 4 g/min biomass and 0.8 g/min catalyst; G.A.: Air; C.G.: H ₂ ; H ₂ flow rate: 1.5 mL/min; in situ catalysis.	Bubbling fluidized-bed reactor	Dry, inert-free, gas composition: H ₂ : 35.41, CH ₄ : 5.09, CO: 36.34, CO ₂ : 23.16	0.97	H ₂ , CO, and CH ₄ fractions increase with catalyst	[79]
Wheat straw	1.80	Metal catalyst Ru/Al ₂ O ₃	T: 550 °C; R.T.: 60 min; Biomass concentration: 20 wt%; Deionized water load: 8 mL; Catalyst concentration: 5 wt%; B.P.S.: <1 mm; C.G.: N ₂ .	Tubular batch reactor	H ₂ : 30.77, CH ₄ : 12.82, CO: 53.85, CO ₂ : 2.56	0.57	N.R.	[45]
Cotton stalks	5.61	Calcined cement kiln dust	T: 800 °C; R.T.: 90 min; Load: 0.5 g dried biomass; G.A.: O ₂ ; in situ catalyst.	Bench-scale fixed-bed reactor	H ₂ : 39.40, CH ₄ : 4.10, CO: 36.80, CO ₂ : 19.70	1.07	H ₂ fraction increases while CH ₄ and CO fractions decrease.	[80]
Corn stalks	4.01	Calcined cement kiln dust			H ₂ : 32.00, CH ₄ : 4.30, CO: 42.00, CO ₂ : 21.70	0.76		[80]
Rice straw	4.15				H ₂ : 26.40, CH ₄ : 6.40, CO: 35.00, CO ₂ : 32.20	0.75		[80]

* VM/FC: Volatile matter/Fixed carbon. T: Temperature. B.P.S.: Biomass particle size. H.R.: Heating rate. R.T.: Reaction time. G.A.: Gasifying agent. G.A./Biomass: Gasifying-agent-to-biomass ratio. C.G.: Carrier gas. N.R.: None reported.

2.1.3. Hydrothermal Carbonization (HTC)

The HTC process has been studied as a promising alternative to upgrading lignocellulosic biomass into hydrocarbons by thermal degradation. This process is attractive due to the possibility of converting wet biomass directly, avoiding drying and saving thermal/electrical energy. In the same way as pyrolysis, solid (so-called hydrochar) and liquid streams are produced. Hydrochar has been studied as a precursor of activated carbon, while the liquid stream has been analyzed as a potential precursor of hydrocarbons [81]. The effects of implementing catalysts in the HTC process have been studied and reviewed. Organic and inorganic catalysts have been reported in the open literature [82]. The objective of catalytic HTC is to increase the hydrochar yield.

Lignocellulosic biomass must be depolymerized, deoxygenated, and carbonized in the HTC process. The organic catalysts used for promoting these reactions are citric acid and acetic acid. The role of these catalysts is to provide a more acidic medium for disrupting cellulose, hemicellulose, and lignin. This organic catalysis increases the hydrochar yield, giving different properties to the product. For instance, the hydrochar properties after acidic catalysis using citric acid differ from those reported when using acetic acid as a catalyst [81,83–85]. Thus, the applications, calorific value, and physical characteristics are different. The same behavior has been identified when using inorganic catalysts such as inorganic acids, salts, and metallic compounds [82]. Hydrochar applications and yields vary depending on the type of catalyst used in the process. For this reason, Djandja et al. [82] revealed that FeCl_3 , HCl, citric acid, some alkalis, and some oxidants are potential candidate catalysts for producing superior solid fuel. In contrast, only organic acids are recommended for producing porous carbon materials.

The operating variables and process conditions are key factors in the HTC process. Temperature, pressure, catalyst loading, solid-to-liquid ratio, and residence time are reported in Table 4. The operating conditions vary depending on the end use of the hydrochar. Nevertheless, most processes are carried out at temperatures higher than 200 °C. Moreover, biochar yield is not always improved when introducing catalysts to the process. There are some cases where the hydrochar quantity decreases after the HTC process. Thus, the effect of the catalyst must be studied based on several experiments and operating conditions to ensure a good performance [86].

Regarding the use of hydrochar, Liu et al. [87] analyzed the application of biochar as an absorbent for heavy metal ions in water and soils and summarized the removal mechanism. A specific case is discussed of treating biochar by steam activation, which performed well in the removal of heavy metals (i.e., Cu^{2+} and tetracycline) at conditions of 500 °C for 45 min. Physicochemical properties of biochar can be modified as described by Chen et al. [88] for the decontamination of aquatic and soil systems by both organic and inorganic pollutants.

The technical, economic, and environmental performance of the HTC process must be analyzed using simulation tools that have been used to assess the feasibility of an HTC plant. For instance, Akbari et al. [89] studied the techno-economic performance of the HTC process applied to yard waste. Two configurations were compared. The first configuration produces biochar using steam and several flash separators, while the second process configuration uses special heat exchangers for increasing temperature. The first configuration was the most promising option from the technical point of view (i.e., mass and energy indicators were higher). Nevertheless, this configuration had the lowest economic performance, with a production cost of 3.3 \$/GJ. On the other hand, the environmental assessment of the HTC process has been reviewed by Hussin et al. [90]. These authors concluded that more studies on the environmental life cycle assessment (E-LCA) of the HTC processes are needed. Furthermore, a lack of comprehensive information on data emissions such as toxic metallic elements and greenhouse gas emissions (GWP) using different types of biomasses through the hydrothermal carbonization process has been evidenced. Thus, the E-LCA of the HTC process can be considered as a research gap for further investigation and development.

Table 4. Catalytic hydrothermal carbonization of lignocellulosic biomass: yields and catalyst effect.

Raw Material	VM/FC *	Catalyst	Operating Conditions	Reactor Type	Hydrochar Yield (wt%)	Catalyst Effect	Ref.
Banana peels	32.60	H ₃ PO ₄ (40 wt%)	T: 230 °C; R.T.: 2 h; Load: 4 g biomass, 50 mL H ₃ PO ₄ solution; B.P.S.: 0.5–1.0 cm; in situ catalysis.	Polytetrafluoroethylene (PTFE) inner steel autoclave	29.17	Hydrochar yield significantly decreases with catalysis.	[91,92]
Wheat straw	7.38	Acetic acid (95 wt%)	T: 200 °C; H.R.: 3 K/min; R.T.: 6 h; Load: 25 g dry biomass, 500 mL feedwater; B.P.S.: 0.5 mm; pH: 2.00; Stirring rate: 90 rpm.	Parr stirred reactor	49.9	Hydrochar yield increases with catalysis.	[93,94]
Wheat straw	7.38	Acetic acid (95 wt%)	T: 260 °C; H.R.: 3 K/min; R.T.: 6 h; Load: 25 g dry biomass, 500 mL feedwater; B.P.S.: 0.5 mm; pH: 2.00; Stirring rate: 90 rpm.	Parr stirred reactor	31.3	Hydrochar yield increases with catalysis.	[95,96]
Glucose	N.A.	Al(OTf) ₃	T: 200 °C; R.T.: 48 h; Load: 1.5 g raw material, 1 mmol catalyst, and 20 mL deionized water; pH: 3.65; R.V.: 50 mL.	Teflon-lined stainless-steel mini autoclaves	31.33	Hydrochar yield decreases and the particle size increases with catalysis.	[97]
Glucose	N.A.	NaOTf	T: 200 °C; R.T.: 48 h; Load: 1.5 g raw material, 1 mmol catalyst, and 20 mL deionized water; pH: 8.92; R.V.: 50 mL.	Teflon-lined stainless-steel mini autoclaves	48.00	Hydrochar yield and particle size increase with catalysis.	[97]
Cellulose	N.A.	Al(OTf) ₃	T: 200 °C; R.T.: 48 h; Load: 1.5 g raw material, 1 mmol catalyst, and 20 mL deionized water; pH: 3.68; R.V.: 50 mL.	Teflon-lined stainless-steel mini autoclaves	38.67	Hydrochar yield decreases and particle size increases with catalysis.	[97]
Cellulose	N.A.	NaOTf	T: 200 °C; R.T.: 48 h; Load: 1.5 g raw material, 1 mmol catalyst, and 20 mL deionized water; pH: 7.58; R.V.: 50 mL.	Teflon-lined stainless-steel mini autoclaves	55.33	Hydrochar yield and the particle size increase with catalysis.	[97]
Hornwort	5.46	KOH	T: 300 °C; R.T.: 30 min; Dilution ratio: 1:8; Load: 30 g biomass, 3 wt% catalyst of initial raw material.	Cylindrical autoclave reactor	31.40	Hydrochar yield decreases with catalysis.	[85]
Metasequoia leaves	11.88	Iron sludge	T: 150 °C; R.T.: 3 h; B.P.S.: 0.15 mm. Load: 5 g biomass, 0.5 g catalyst, and 60 mL deionized water; Stirring time: 0.5 h, in situ catalysis.	Enclosed stainless-steel reactor	59.53	Hydrochar yield increases with catalysis.	[98]
Wooden stir sticks (white pine and birch)	6.76	Acid catalyst solution	T: 240 °C; H.R.: 7 °C/min; R.T.: 1 h; Load: 10 g biomass, 120 mL water and catalyst; C/B: 12/1; B.P.S.: 2 mm; in situ catalysis.	Parr bench-top reactors	45.50	Hydrochar yield increases with catalysis.	[95,96]
Rice husk	5.00	NaCl (Analytical-grade)	T: 220 °C; R.T.: 60 min; Load: 7.5 g biomass, 22.5 mL deionized water, and NaCl was 5% of mass of rice husk; B.P.S.: 0.6 mm; Ultrasonic pretreatment was implemented with 260 W.	Stainless-steel batch reactor	65.00	Hydrochar yield decreases with catalysis.	[43,99]

Table 4. Cont.

Raw Material	VM/FC *	Catalyst	Operating Conditions	Reactor Type	Hydrochar Yield (wt%)	Catalyst Effect	Ref.
Sugarcane bagasse	5.94	HCl	T: 180 °C; R.T.: 4 h; B.P.S.: <1 mm; Biomass loading: 12 g; 100 mL HCl; HCl concentration: 2 M; For adsorption: pH 5.00 and stirring rate 200 rpm.	Stainless-steel Teflon-line autoclave reactor	49.70	N.R.	[77,100]
Cassava pulp	7.96	Acetic acid (Dehydration catalyst)	T: 220 °C; H.R.: 6 °C/min; R.T.: 5 h; P: 30 bar; Load: 350 mL sludge; Sludge/Raw material: 1/1 (wt%).	Stainless-steel high-pressure reactor	69.8	Hydrochar yield increases with catalysis.	[101]
Cotton textile waste	14.95	FeCl ₃ ·6H ₂ O	T: 240 °C; H.R.: 5 °C/min; R.T.: 4 h; Load: 3 g biomass, 1 g FeCl ₃ , and 60 mL deionized water; B.P.S.: 1 mm.	Non-stirred stainless-steel Teflon-lined reactor	21.95	Hydrochar yield decreases with catalysis.	[102]
Avocado peel	2.24	FeCl ₃ ·6H ₂ O	T: 180 °C; H.R.: 4 °C/min; R.T.: 5 h; Load: 100 g biomass, 600 mL deionized water; C/B: 20 wt%; B.P.S.: 0.3 mm.	High-pressure stirred laboratory reactor	62.7	Hydrochar yield increases with catalysis.	[103]

* VM/FC: Volatile matter/Fixed carbon. T: Temperature. P: Pressure. B.P.S.: Biomass particle size. H.R.: Heating rate. R.T.: Reaction time. R.V.: Reaction volume. C/B: Catalyst-to-biomass ratio. N.A.: Does not apply. N.R.: None reported.

2.2. Catalytic Biomass Fractionation

Lignocellulosic biomass fractions have been researched and studied for producing a series of value-added products and energy vectors based on biotechnological pathways. These conversion routes require a pretreatment stage for disrupting biomass materials and increasing access to enzymes and microorganisms. Catalytic biomass upgrading refers to using any catalyst (homogeneous or heterogeneous) for the disrupting and upgrading of biomass components into platform molecules and value-added products.

Catalysis is present in the pretreatment of biomass. Chemical pretreatment methods are considered catalytic methods for disrupting biomass. The acid pretreatment uses inorganic and organic acids as catalysts, the ammonia fiber expansion (AFEX) pretreatment uses ammonia as catalysts, alkaline pretreatment uses inorganic bases for removing lignin, and the organosolv pretreatment uses an inorganic acid and alcohol to separate the three biomass fractions [104,105]. Therefore, all these methods are the subject of study for finding new and improved catalysts and reactions in order to increase yields and productivity. One of the most important drawbacks of the pretreatment methods is the use of homogeneous catalysts, as liquid waste streams with the catalysts are generated [106]. This drawback encourages using new catalysts for the pretreatment, increasing operational expenditures.

For instance, the acid pretreatment uses sulfuric acid (or any other inorganic acid) to remove the hemicellulose content of a biomass sample. The sulfuric acid is not recovered after the pretreatment stage for further use [107]. Therefore, the pretreatment requires a constant feed flow of a sulfuric acid solution to pretreat new biomass. This issue can be overcome by implementing solid catalysts in the pretreatment stage. Indeed, zeolites and cation-exchange resins have been researched as possible catalysts for the acid pretreatment of biomass [106]. However, few studies have reported the use of solid catalysts instead of homogeneous catalysts due to the cost associated with the use of the catalyst. Even so, solid catalysts in biomass pretreatment could help to improve the environmental performance due to the recyclability and re-use potential of this kind of compounds.

The pretreatment stage has been considered a key step for biomass upgrading, as this stage allows decreasing crystallinity and biomass recalcitrance [106]. After this process, enzymatic hydrolysis is carried out to produce reducing sugars from the cellulose fraction (i.e., glucose). This step can also be considered as a catalytic process, as the enzymes are the medium for obtaining the desired product. After this process, biotechnological routes are applied to upgrade these sugars to value-added products through fermentative processes. The product portfolio of biotechnological conversion is wide, as several microorganisms can upgrade glucose to different products. Indeed, the lignocellulosic fractions can be upgraded into different valuable products with a solid catalyst. Table 5 presents some interesting products obtained after the direct upgrading of biomass in the presence of a metal catalyst.

Table 5. Conversion of main biomass fractions into value-added products via catalytic processes.

Fraction	Biomass	Catalyst	Product	Operating Conditions	Reactor Type	Yield (wt%)	Ref.
Cellulose	Corn stover	Al ₂ (SO ₄) ₃	Methyl levulinate	T: 170 °C; R.T.: 45 min; B.P.S.: 1 mm; Cellulose load: 0.4 g; Solvent: Methanol; Stirring rate: Low level; Microwave power: 800 W; Solvent load: 15 mL.	Microwave reactor	84.49	[108]
	N.R.	RuCl ₃	5-Hydroxymethylfurfural (5-HMF), lactic acid (Lac), and levulinic acid (LA)	T: 220 °C; R.T.: 30 min; Cellulose concentration: 4 wt%; Solvent: Butanol; Catalyst concentration: 0.125 mol/L	High-pressure reactor	5-HMF: 83.30 Lac: 2.65 LA: 14.05	[109]
	Sugarcane leaf waste	FeCl ₃	Reducing sugars	T: 60 °C; R.T.: 3.5 min; pH: 4.8; Catalyst concentration: 2 M; Microwave power: 700 W; B.P.S.: <1 mm; Biomass load: 5 g.	Microwave oven	40.6	[110]
	Food waste (Cooked rice and bread crust)	SnCl ₄	Hydroxymethylfurfural (HMF) and glucose	T: 140 °C; R.T.: 20 min; Catalyst concentration: 20 mol%.	Microwave reactor	HMF: 9.50 Glucose: 90.50	[111]
	Corn stover	1-(1-propylsulfonic)-3-methylimidazolium chloride	Reducing sugars	T: 160 °C; R.T.: 3 h; B.P.S.: 0.7 mm; Biomass load: 0.05 g; Catalyst load: 2.50 mL.	Stainless-steel reactor	90.20	[112]
Hemicellulose	Rice straw	CuO	Xylose and arabinose	T: 160 °C; R.T.: 3 h; Stirring rate: 600 rpm; P _{H2} : 1.5 MPa; B.P.S.: 0.062 mm; C.P.S.: 0.075 mm; C/B: 3/10 (wt%).	Stainless-steel reactor	Xylose: 53.00 Glucose: 17.30	[113]
	Corn cob	NaHCO ₃	Glucose	T: 50 °C; Biomass load: 1 g; pH: 5.0; Stirring rate: 200 rpm; Catalyst concentration: 2 wt%.	Rotary shaker	Glucose: 67.60	[114]
Hemicellulose	Beech wood	SnCl ₄	Furfural and xylose	T: 150 °C; R.T.: 120 min; Load: 0.1 g xylan, 0.1 mmol catalyst, 5 mL ultrapure water; Solvent: 2-methyltetrahydrofuran; (2-MTHF); MTHF/water: 2/5 vol%.	Batch reactor	Furfural: 78.1 Xylose: 8.30	[115]
	<i>Cannabis sativa</i> L. shives	Al ₂ (SO ₄) ₃	Furfural	T: 160 °C; R.T.: 90 min; Catalyst concentration: 5 wt%; Biomass load: 1200 g.	Bench-scale reactor	62.70	[116]
	<i>Typha latifolia</i>	MgCl ₂	Xylose and glucose	T: 180 °C; R.T.: 15 min; B.P.S.: 1 mm; Catalyst concentration: 0.4 M.	Batch reactor	Xylose: 90.60 Glucose: 61.70	[117]

Table 5. Cont.

Fraction	Biomass	Catalyst	Product	Operating Conditions	Reactor Type	Yield (wt%)	Ref.
Lignin	Corncob	ZnMoO ₄ /MCM-41 (MCM-41: 1.5 g)	Ethyl coumarate (EC) and ethyl ferulate (EF)	T: 220 °C; R.T.: 4 h; P _{H₂} : 30 atm; Solvent: Ethanol; Lignin load: 100 g; Catalyst load: 25 mg; Solvent load: 15 mL.	Parr autoclave reactor	EC: 3.90 EF: 3.70	[118]
	Birch	Ni-Fe/AC (Ni/Fe: 1/1)	Propylsyringol	T: 200 °C; R.T.: 6 h; P _{H₂} : 2 MPa; Stirring rate: 800 rpm; Solvent: Methanol; Lignin load: 100 mg; Load: 50 mg catalyst; 10 mL solvent.	Parr reactor	20.30	[119]
	Sugarcane bagasse	Ni/ZrP (Ni: 20 wt%)	4-Ethyl phenol	T: 270 °C; R.T.: 4 h; P _{H₂} : 2 MPa; Stirring rate: 650 rpm; Solvent; Isopropanol; Lignin load: 0.5 g; Load: 0.1 g catalyst; 20 mL solvent.	Stainless-steel autoclave	7.39	[120]
	Hardwood	Cu/Mo-ZSM-5	Phenol, 3-methoxy,2,5,6- trimethyl (PMT)	T: 220 °C; R.T.: 7 h; Inert atmosphere; Solvent: Methanol; Lignin load: 0.5 g; Load: 0.125 g catalyst, 60 mL solvent, 1.7 mmol NaOH; Water/Methanol: 45/15 (vol%).	Parr reactor	20.60	[121]
	Wheat straw	Ga(OTf) ₃	Soluble phenolic compounds	T: 160 °C; R.T.: 2 h; Solvent: Ethanol; Lignin load: 40 g; Catalyst concentration: 8 mmol/L.	Autoclave reactor	17.90	[122]

T: Temperature. P_i: Pressure of component i. B.P.S.: Biomass particle size. C.P.S.: Catalyst particle size. R.T.: Reaction time. C/B: Catalyst-to-biomass ratio. N.R.: None reported.

Cellulose can be degraded to 5-hydroxymethyl furfural (5-HMF) as reported by Jiang et al. [123], formic acid, levulinic acid, ethylene glycol, gluconic acid, lactic acid, sorbitol, and mannitol. The operating conditions and catalyst type vary according to the desired product. For instance, lactic acid has been produced using cellulose as raw material, reaching a conversion yield of about 90 wt% in a stirred tank reactor at lab scale at 240 °C, 2 MPa, 600 rpm, and 30 min in the presence of ErCl_3 [124]. Gluconic acid was produced with a yield from 30–50 wt% when using a homogeneous catalyst (FeCl_3) for producing gluconic acid at 110 °C, 600 rpm, and 120 min [125]. On the other hand, hemicellulose can be upgraded to furan-based components and lactones after depolymerization, dehydration, and deoxygenation. Finally, catalytic lignin decomposition allows the production of phenolic compounds such as vanillin, ethyl coumarate, and ethyl ferulate. All these processes occur at high temperature and pressures ($T > 100$ °C, and $P > 2$ MPa). Therefore, heating and power requirements of catalytic upgrading of biomass can be hotspots of these processes. The research on high-selectivity catalysts is crucial for reducing the downstream processing as much as possible to obtain a high-purity value-added product. Table 5 shows different metal catalysts used for biomass upgrading. Nevertheless, few studies have been focused on analyzing the recyclability and re-use potential of these catalysts from a techno-economic and environmental perspective. Thus, more studies considering this point are required.

On the other hand, platform molecules are derived after disrupting the lignocellulosic matrix of biomass. The United States Department of Energy (USDOE) has proposed a list of the top 12 biochemicals/platforms produced from biomass [126]. Most of these compounds are produced from C_5 and C_6 sugars (i.e., xylose and glucose) via catalytic upgrading or fermentation pathways. Indeed, aqueous solutions of monomeric sugars derived from biomass could be subjected to various types of reactions involving oxygen removal and C–C bonds formation. Therefore, the production of highly reactive molecules to be transformed into a wide variety of compounds is only possible through hydrolysis-based methods [2]. The main platform molecules derived from hydrolytic processing are furfural, hydroxymethylfurfural (HMF), levulinic acid, and γ -valerolactone.

To develop a suitable mixture of liquid fuels for usage or blending with commercial fuels such as gasoline (C_5 – C_{12}), jet fuel (C_9 – C_{16}), and diesel, the furan platform has been studied as a potential precursor of these hydrocarbons. Furan-based compounds are produced via dehydration and deoxygenation of sugars (e.g., xylitol, glucose). Inorganic acid or ionic liquids are used in homogeneous catalysis to produce furfural and HMF. Furfuryl alcohol, cyclopentanol, n-pentane, butane, furan, 2,5-dimethyl furan (DMF), and tetrahydrofurfural (THF2A) are a few of the key products that can be obtained from furan compounds [2]. Several reviews have dedicated efforts to giving comprehensive information about the possible applications of furan-based compounds (i.e., furfural and HMF) and their conversion pathways into high-value-added products [104,105,127].

Another platform generated from the hydrolysis of lignocellulosic biomass is levulinic acid. This organic acid is esterified to produce ethyl and methyl esters, which are then combined with diesel fuel. However, levulinic acid can be upgraded to γ -valerolactone through the dehydration of the angelica lactone pathway using homogeneous or heterogeneous catalysis. Subsequently, γ -valerolactone can be upgraded to added-value chemicals such as 5-nonanone through the pentenoic acid hydrogenation pathway or transformed into methyl-tetrahydrofuran, which is a gasoline additive. Moreover, levulinic acid can be used as a polymer additive [128]. Another way to produce additives for fuels or even other added-value chemicals is through the direct catalytic conversion of biochemical products. Among the main products obtained by biochemical routes, lactic acid has been one of the most researched. Lactic acid can be transformed using heterogeneous catalyst in light alkanes such as methane, ethane, and propane [129]. Further, lactic acid can be transformed into C_6 and C_7 ketones. Moreover, lactic acid can be upgraded to polylactic acid using heterogeneous catalysts. This process is described by Ortiz-Sanchez et al. [130], where SnO is required as solid catalyst. Nevertheless, other catalysts need to be researched

to improve the process, as SnO suffers deactivation in the presence of water. Thus, a high-efficiency removal system must be designed for avoiding low yields and productivities. Finally, glycerol (a by-product of the biodiesel production) has been studied to be upgraded via heterogeneous catalysis. Indeed, this molecule has been upgraded to produce 1,2-propanediol and 1,3-propanediol via hydrogenolysis, dihydroxyacetone via oxidation, and other value-added products via etherification and esterification [131]. A brief list of the possible value-added products derived from the furan platform, lactic acid, levulinic acid, and glycerol is presented in Table 6.

Regarding the aqueous phase derived from biomass, Pipitone et al. [132] have studied different catalytic valorization techniques through reforming processes to produce H₂ from the oxygenated compounds present in this phase. The authors analyzed the available routes for the catalyst synthesis that allowed high selectivity, substrate conversion, and industrial scaling. Morales et al. [133] reported the production of H₂ with a yield of 85% from glycerol by the aqueous-phase reforming process using nickel aluminate catalyst (0.5 g) at 250 °C and 45 bar with a composition of 10 wt% glycerol solution. Moreover, heterogenous catalysis can be applied to biomass-derived aqueous phase for the obtaining of high-valued-added products such as platform chemicals through dehydration, hydrogenation, oxidation, and reforming reactions, as previously mentioned [134].

3. Recent Trends Related to Catalytic Processes for Improving Biorefineries' Designs

Catalytic upgrading of biomass has increased in recent years in order to obtain more bio-based products that can be used in any productive sector. Therefore, different research efforts have been focused on analyzing new ways to implement catalytic processes for biomass upgrading or waste-streams valorization [135–138]. This review paper refers to some trends related to the catalytic upgrading of bio-based compounds. However, there are more trends worthy of being studied and analyzed. The trends presented are as follows: biocatalysis, CO₂-upgrading, catalysts' recyclability and use, and biochar as catalysts' source. The above-mentioned research lines in catalytic processes aim to improve biorefineries' designs, as more products can be involved in a biorefinery. Moreover, the sustainability of these facilities is upgraded due to the emissions reduction and waste-streams minimization.

Table 6. Products derived from platform molecules: 5-HMF, furfural, lactic acid, levulinic acid, and glycerol.

Platform Molecule	Catalyst	Product	Operating Conditions	Reactor Type	Yield (wt%)	Catalyst Effect	Ref.
HMF	Perovskite-Type Oxide (PTO) supported by Ni: LF-N5 (5 wt% Ni)	2,5-Dimethylfuran (DMF), 5-Methylfurfuryl alcohol (MFA) and 5-Methylfurfural (MF)	T: 230 °C; R.T.: 6 h; Load: 1.0 mmol HMF, 1.0 mmol n-tetradecane, 100 mg catalyst, 12 mL ethanol; P _{H2} : 5.0 MPa.	Parr reactor and magnetic stirrer	DMF: 69.30, MFA: 28.80, MF: 1.90	DMF yield increases while MFA and MF decrease.	[139]
	Mg:Al:Ni (2 mole ratio; 48.3 wt% Ni)	Furfuryl alcohol (FOL)	T: 180 °C; P: atmospheric; R.T.: 10 h; Load: 1 mL catalyst.	Vertical down-flow fixed-bed reactor	FOL: 93.99	N.R.	[140]
	Pt/MCM-41 (1 wt% Pt)	2,5-bis-(hydroxymethyl) furan (BHMF) and 5-Methylfurfuryl alcohol (MFA)	T: 35 °C; R.T.: 2 h; Catalyst/HMF (wt): 1/5; Water: 2 mL; P _{H2} : 0.8 MPa.	Batch reactor	BHMF: 98.9, MFA: 1.10	N.R.	[141]
	Pd/SiO ₂ (0.6) + Ir-ReO _x /SiO ₂ (5–2.5)	1,6-Hexanediol, 1,5-Hexanediol, Hexane, 1-Hexanol, and 2,5-bis(hydroxymethyl) tetrahydrofuran	T: 100 °C; P _{H2} : 5 MPa; Load: 1 wt% HMF, 1.0 g Pd/SiO ₂ in upper layer and 1.0 g; Water/THF: 2/3 (vol%).	Fixed-bed reactor	1,6-HDO: 46.20, 1,5-HDO: 19.40, Hexane: 12.90, 1-Hexanol: 17.50, DHMTHF: 4.70	N.R.	[142]
	C-Fe ₃ O ₄ -Pd	2,5-furandicarboxylic acid (FDCA), 2,5-diformylfuran (DFF), and 2-hydroxymethyl-furan-5-carboxylic acid	T: 80 °C; R.T.: 4 h; Solvent: H ₂ O; Load: 50.4 mg HMF, 8 mL solvent, and 40 mg catalyst; O ₂ flow rate: 30 mL/min.	N.R.	FDCA: 82.30 DFF: 1.20 HMFA: 0.9	N.R.	[143]
Levulinic acid	Beta zeolite (H-Beta-19, Si/Al: 23)	Diphenolic acid (DPA)	T: 140 °C; R.T.: 4 h; Load: 12 mmol Levulinic acid, 0.3 g catalyst; Phenol/Levulinic acid: 6 (mol).	Pressure glass reactors	DPA: 45.70	N.R.	[144]
	Ni/Al ₂ O ₃ (35 wt% Ni)	2-methyltetrahydrofuran (MTHF) and γ-valerolactone (GVL)	T: 250 °C; R.T.: 5 h; P _{H2} : 70 bar; Solvent: 2-propanol; Load: 5 wt% levulinic acid in solvent; Levulinic acid/catalyst: 10 (wt%).	Autoclave reactor	MTHF: 75.00, GVL: 8.00	Products yields increases with catalysis.	[145]
	Pd/HZSM-5 (2 wt% Pd)	Valeric acid and its esters (VA + VE)	T: 240 °C; R.T.: 8 h; P _{H2} : 4.0 MPa; Solvent: Ethanol.	Stainless-steel batch reactor	VA + VE: 92	N.R.	[146]
	CuMg (Cu ²⁺ : 0.25 mol/L; Mg ²⁺ : 0.5 mol/L)	1,4-pentanediol (PDO)	T: 170 °C; R.T.: 2 h; P _{H2} : 3 MPa; Stirring rate: 400 rpm; Load: 40 mg catalyst, 40 mg levulinic acid, and 3.96 g ethanol.	Autoclave reactor	PDO: 53.6	N.R.	[147]
	Amberlyst-15	Succinic acid (SA), maleic acid (MA), fumaric acid (FA), and furoic acid (FuA)	T: 80 °C; R.T.: 24 h; Stirring rate: 500 rpm; Oxidant: H ₂ O ₂ ; Solvent: Water; Load: 50 mg catalyst, 1 mmol furfural, 30% oxidant, and 3 mL solvent.	Schlenk glass tube attached with a reflux condenser	SA: 74, MA: 11, FA: <1, FuA: 2	Catalysis is needed for production.	[148]

Table 6. Cont.

Platform Molecule	Catalyst	Product	Operating Conditions	Reactor Type	Yield (wt%)	Catalyst Effect	Ref.
Furfural	NiO-MgO Ni/Mg: 0.25 mol%	Furan	T: 190 °C; R.T.: 5 h; Solvent: Cyclopentylmethyl ether; H ₂ : furfural molar ratio: 11.5; Furfural flow rate: 2.3 mmol/h; H ₂ flow rate: 10 mL/min.	Tubular quartz reactor	Furan: 88	N.R.	[149]
	NiO-MgO Ni/Mg: 0.25 mol%	Furfuryl alcohol	T: 190 °C; R.T.: 5 h; Solvent: Cyclopentylmethyl ether; H ₂ : furfural molar ratio: 11.5; Furfural flow rate: 2.3 mmol/h; H ₂ flow rate: 10 mL/min.	Tubular quartz reactor	Furfuryl alcohol: 6	N.R.	[149]
	1,8-diazabicyclo [5.4.0] undec-7-ene (Substrate/Catalyst: 5.56)	Furoic acid	T: 40 °C; R.T.: 4 h; P _{O₂} : 0.1 MPa; Load: 48 mg furfural, 2 mL DMSO, 30 mg catalyst.	Teflon-lined stainless-steel autoclave	Furoic acid: >99	Catalysis is needed for production.	[150]
	5 wt% Ru/C	1,4-butanediol (BDO), tetrahydrofuran (THF), and n-butanol (NBA)	T: 170 °C; P: 50 bar; R.T.: 3 h; Load: 16 g furan, 45 g water, 51 g ethanol, 0.1 g catalyst; Ru/C: 1/12.5 and Furan/H ₂ O: 1/12.5.	16-reactor nanoflow unit	BDO: 21, THF: 52 NBA: 14	N.R.	[151]
	Ru/SiO ₂	Furfurylamine	T: 130 °C; P _{H₂} : 750 psi; R.T.: 10 h; Dioxane/water: 40:1 (%wt); Furfural concentration: 0.1 M; 40 mL water.	Batch reactor	Furfurylamine: 58	Catalysis is needed for production.	[152]
Lactic acid	Magnesium aluminate spinel (Mg/Al: 1/2 mol%)	Acetaldehyde (AD), propionic acid (PA), acetic acid (ACA), acrylic acid (AA), and 2,3-pentanedione (PD)	T: 380 °C; Feedstock: 20 wt% solution of lactic acid; Catalyst load: 0.38 mL; Solvent: water; C.G.: N ₂ ; Feed flow rate: 1 mL/h.	Fixed-bed quartz reactor	AD: 87.5, PA: 2.6 ACA: 1.7, AA: 5.5 PD: 1.0	N.R.	[153]
	ZSM-5 zeolite (Alkali-treated with 0.5 mol% NaOH)	Acrylic acid	R.T.: 350 °C; Catalyst load: 1.5 g; LHSV: 4.0 h ⁻¹ .	Vertical fixed-bed steel reactor	Acrylic acid: 64.8	N.R.	[154]
	3Pb-1Pt (Carbon black catalyst)	Pyruvic acid (PA) and acetic acid (AA)	T: 90 °C; P: 0.1 MPa; R.T.: 20 min; pH: 12; Catalyst load: 0.25 g; Load: 25 g lactic acid, 0.21 g LiOH·H ₂ O (90 wt%); O ₂ flow rate: 100 mL/min; Stirring rate: 800 rpm.	Three-neck flask	PA: 59.98, AA: 1.05	Catalysis is needed for production.	[155]
	H ₃ PW on activated carbon (30 wt% H ₃ PW)	Polylactic acid	T: 160 °C; R.T.: 4 h; Catalyst load: 0.02 g; Stirring rate: 240 rpm.	50-mL three-neck round-bottom flask	Polylactic acid: 60.00	N.R.	[156]
	Cs-doped hydroxyapatite catalyst (Ca/Cs: 1.622/1.667 mol)	2,3-Pentanedione	T: 300 °C; R.T.: 4.5 h; Catalyst load: 0.38 mL; Calcination temperature: 700 °C; C.P.S.: 0.40 mm; C.G.: N ₂ ; N ₂ flow rate: 1 mL/min; Feed flow rate: 1 mL/h; Lactic acid feedstock: 20 wt% in water.	Fixed-bed quartz tubular reactor	2,3-Pentanedione: 63.8	Catalysis is needed for production.	[157]

Table 6. Cont.

Platform Molecule	Catalyst	Product	Operating Conditions	Reactor Type	Yield (wt%)	Catalyst Effect	Ref.
Glycerol	Nb-MgAl (18 wt% Nb)	Diglycerol (DG) and formic acid (FA)	T: 150 °C; Glycerol concentration: 4.31×10^3 mol/L; Continuous process.	Stainless-steel packed-bed reactor	DG: 66.50, FA: 23.75	Only formic acid is produced.	[158]
	NiAl-Glycerinate (Prepared by two-step calcination and 10 wt% CeO ₂)	Hydrogen	T: 630 °C; Water/Glycerol: 9 mol%; Catalyst load: 0.5 g; Gas Hourly Space Velocity (GHSV) of $19,600 \text{ cm}^3 \text{ gcat}^{-1} \text{ h}^{-1}$.	Fixed-bed tubular stainless-steel reactor	Hydrogen: 77	Hydrogen yield increases with catalysis.	[159]
	NS-ZM-75 (Si/Al: 75)	Acrolein and acetol	T: 320 °C; R.T.: 24 h; P: 1 atm; Glycerol concentration in feed: 5 wt%; Coke: 0.130 mg/g _{cat} .	Stirred laboratory reactor	Acrolein: 92, Acetol: 4	N.R.	[160]
	Pt-Bi/AC (5 wt% Pt and 1.5 wt% Bi)	Dihydroxyacetone (DHA), glyceric acid (GCA), and tartronic acid (TTA)	T: 80 °C; P _{O₂} : 3.5 bar; R.T.: 2 h; Stirring rate: 800 rpm; Glycerol initial concentration: 1 M; Glycerol/dry catalyst: 10 wt%; Load: 100 mL glycerol solution and 0.92 g catalyst.	Stainless-steel batch reactor	DHA: 35.28, GCA: 6.72, TTA: 10.92	N.R.	[161]
	Ce _{0.75} Zr _{0.25} O ₂ (Ce/Zr: 3/1 wt%)	Glycolic acid	T: 60 °C; NaOH/glycerol: 2(mol%); O ₂ /glycerol: 0.23(mol%); Catalyst/glycerol: 0.77(wt%); Glycerol concentration: 2 M.	Stirred batch reactor	Glycolic acid: 68	N.R.	[162]

T: Temperature. P: Pressure. P_i: Pressure of component i. C.P.S.: Catalyst particle size. R.T.: Reaction time. C.G.: Carrier gas. N.R.: None reported.

3.1. Biocatalysis as the Basis for Producing Specialty and Fine Chemicals

Biocatalysis is a new alternative that several industrial processes are implementing to assist or replace existing synthetic routes through which specialty and fine chemicals are produced [163]. Therefore, the use of cell systems or enzymes has mainly been studied specifically to cover the demands of pharmaceutical applications to obtain high-value compounds. The current technologies are based on the production of optical purity species for the required chiral center that represents a specific function in a medical patient [164]. Moreover, several authors have implemented green chemistry metrics to study the optimum operating conditions to allow the minimum waste generation and use of hazardous reagents or solvents [165].

The use of a biocatalyst involves economic factors that must be considered during the process. According to Pollard et al. [164], the obtained products must present considerably similar concentrations of those products generated when using chemical standard routes. Nevertheless, enzymes need to work in high-substrate concentrations without decreasing the activity. The second aspect that conditions the productive process is the biocatalyst cost, and this metric must be at a value around $1000 \text{ g}_{\text{product}}/\text{g}_{\text{enzyme}}$ activity for the enzymes and at around $15 \text{ g}_{\text{product}}/\text{g}_{\text{biocatalyst}}$ for the cell systems.

Table 7 summarizes fine compounds obtained when using biocatalysts in different substrates, as well as the application of each precursor for the synthesis of a specific pharmaceutical product. Ketone is the most common substrate and is used for the obtaining of pyrimidines and chiral intermediates. According to Chong et al. [166], the inhibitor ipatasertib can be efficiently synthesized by bicyclic pyrimidine as the starting material of the Ketoreductase enzyme (KRED) that acts on the ketone. This compound is produced with a yield of 86.00 wt%, and as reported, the operating conditions in terms of temperature and pH are neutral or not highly energy demanding for the biocatalytic asymmetric reduction that occurs. When comparing to chemical routes, the use of extreme conditions can cause isomerization, rearrangement of the compound, or racemization [167]. These phenomena reduce the productivity and make upstream processing necessary in order to reach purity and demanded standards.

Pollard et al. [164] note that biocatalytic processes are carried out in small scales when compared to most of the existing chemical processes. Up to 10,000 tons of pharmaceutical compounds are produced per year, and the scaling-up from laboratory scale is difficult. Factors such as batch operating mode can represent a negative effect for the enzyme or cell systems, as the substrate consumption has repercussions on the product quality standards [168]. Moreover, the large capacity of the devices at industrial level does not allow a perfect mixing, or if so, the energy consumption is higher than that at laboratory scale. Finally, the equipment materials are not the same when referring to one scale or another, which leads to low productivities [164].

Enzymes promote stability and selectivity for the desired compound [167]. For instance, when using Cyclohexanol as substrate and KRED as enzyme, St-Jean et al. [169] described that for a thermal requirement of 50 °C in an advanced racemic intermediate, the process reaches a yield of 95.00 wt% for diketone intermediate, an intermediate for the synthesis of Navoximod (II) as an IDO inhibitor.

Several mental health diseases such as anxiety and depression are treated with medicine that causes side-effect profiles. Nevertheless, (R)-sec-Butylamine 17 and (R)-1-cyclopropylethylamine constitute chiral intermediates from which Corticotropin-Releasing Factor-1 (CRF-1) can be synthesized as a receptor antagonist [164]. As shown in Table 7, another receptor antagonist can be synthesized from 3-Fluoro-4-aminopiperidine, produced by the asymmetric transaminase [170]. The reaction time indicates that the product is obtained after 24 h; however, the yield is 94.00 wt%, and the operation is under mild conditions.

Table 7. Biocatalysis applied to upgrade bulk products into high-value-added products.

Substrate	Microorganism/Enzyme	Product	Operating Conditions	Yield (wt%)	Application	Ref.
Ketone	Ketoreductase enzyme (KRED ^{Comm} : 3 wt%)	Bicyclic pyrimidine	T: 30 °C; pH: 7.0 phosphate buffer; Substrate concentration: 105 g/L; NADP: 0.1 wt%; Reductant: 2-propanol.	86.00	Synthesis of inhibitor ipatasertib that targets the Akt kinase (ATP-binding).	[166]
Cyclohexanol	Ketoreductase enzyme (KRED ^{Comm} : 0.5 wt%)	Diketone intermediate	T: 50 °C; pH: 7.2 phosphate buffer; Substrate concentration: 100 g/L; Reductant: 2-propanol.	95.00	Synthesis of Navoximod (II) as an IDO inhibitor.	[169]
Ketone	Alcohol dehydrogenase (ADH ^{Comm} : 0.4 wt%)	Hydroxy ester intermediate	T: 30 °C; pH: 7.0 potassium phosphate buffer; R.T.: 18 h; Ketone concentration: 2 mg/mL; Enzyme concentration: 2 mg/mL.	88.00	Synthesis of a Gamma secretase inhibitor.	[166]
Tetralone	Asymmetric transaminase (ATA ^{Comm} : 0.4 wt%)	Chiral amine intermediate	T: 30 °C; pH: 7.8 phosphate buffer; R.T.: 24 h; Substrate concentration: 10 mg/mL; Enzyme mass: 30 mg; Cosolvent: Methanol (3.3 wt%).	94.00	Synthesis of a Gamma secretase inhibitor.	[171]
Ketone	Asymmetric transaminase (ATA ^{Comm} : 2 wt%)	3-Fluoro-4-aminopiperidine	T: 45 °C; pH: 10.5 with 0.85 M borate buffer; R.T.: 24 h; Substrate concentration: 10 mg/mL; Enzyme concentration: 1 g/mL; DMSO: 20 vol%; N ₂ sweep was carried out.	94.00	Synthesis of a CGRP receptor antagonist.	[170]
Ketone	Asymmetric transaminase (ATA ^{Eng} : 1 wt%)	Chiral amino-acid intermediate	T: 65 °C; R.T.: 24 h; Substrate concentration: 75 g/L; Enzyme loading: 1 wt%; Without organic cosolvent.	89.00	Synthesis of Sacubitril for heart failure treatment.	[172]
Aldehyde: Racemic amine tranylcypromine sulfate 1 (rac-trans)	Imine reductase (IR-46: 1.2 wt%)	Amine tranylcypromine sulfate 1 (1R,2S)	T: 30 °C; pH: 6.3 with NaOAc buffer; Substrate concentration: 10.5 g/L; Enzyme loading: 453.7 (wt%).	84.00	Synthesis of lysine-specific demethylase-1 inhibitor GSK2879552.	[173]
Isopropyl ester	<i>Streptomyces purpureus</i> (RedAm ^{Eng} : 1.5 wt%)	Propan-2-yl (1S,3S)-3-(Methylamino) cyclobutane-1-carboxylate butanedioic acid (1:1)	T: 25 °C; R.T.: 72 h; pH: 7.2 with potassium phosphate buffer; Substrate load: 5.0 g; Enzyme loading: 125 mg; DMSO: 2.5 mL.	73.00	Synthesis of abrocitinib JAK1 inhibitor.	[174]

Table 7. Cont.

Substrate	Microorganism/Enzyme	Product	Operating Conditions	Yield (wt%)	Application	Ref.
Ketone	Nitrilase enzyme (Nitrilase ^{Comm} ; 5 vol%)	Bicyclic pyrimidine	T: 25 °C; pH: 7.2 with 0.5 M K ₂ SO ₄ /50 mM KH ₂ PO ₄ buffer; Substrate concentration: 20 wt%; Without organic cosolvent.	45.00	Synthesis of the Akt kinase inhibitor ipatasertib (I).	[166]
Vinyl acetate	Lipase from <i>Pseudomonas fluorescens</i>	<i>rac</i> -phenylethanol	T: 40 °C; R.T.: 48 h; Stirring rate: 250 rpm.	94.00	For ophthalmic preservations and used as an inhibitor of cholesterol absorption.	[175]
Racemic mandelic acids	<i>E. coli</i> TCD04 containing pET28a- <i>ArMR</i>	Phenylglyoxylic acid	T: 30 °C; R.T.: 48 h; Fermentation volume: 100 mL; No addition of coenzyme or cosubstrate.	99.00	Synthesis of food additives and pharmaceutical intermediates.	[176]
Ketones	ω -Transaminases from <i>Ochrobactrum anthropi</i>	(1S)-1-phenylethylamine	pH: 7.0 with phosphate buffer 50 mM; R.V.: 2 mL; Enzyme concentration: 5 mg/mL; DMSO: 15 v/v%.	94.00	Used as a sacrificial chiral auxiliary for diastereoselective additions.	[177]
Racemic mandelonitrile	Nitrilase BCJ2315 from <i>Burkholderia cenocepacia</i> J2315	(R)-(-)-mandelic acid	T: 30 °C; pH: 8.0 with sodium hydroxide 6 M; Substrate concentration: 150 mM; R.T.: 70 min; Stirring rate: 250 rpm; Enzyme load: 1 g.	97.40	Synthesis of penicillin and cephalosporin.	[178]
Glycosynthase	exo-Hexosaminidase	Lacto-N-triose II	T: 37 °C; pH: 7.5; R.T.: <1 h; Stirring rate: 650 rpm; Lactose concentration: 600 mM; DMSO: 20 wt%. Catalyst load: 11 g/kg product.	90.00	Synthesis of human milk oligosaccharides and own nutraceutical potentials.	[179]

T: Temperature. R.T.: Reaction time. R.V.: Reaction volume.

The implementation of a biocatalytic route in a productive process might demand specificity related to the equipment and a considerable economic investment. Nevertheless, the operating conditions indicate that biocatalysis is a promising alternative for the synthesis of fine chemicals, especially those related to the pharmaceutical sector, where productivity and selectivity constitute key factors [180]. Additionally, there is a great variety of enzymes and cell systems available for each compound, which contributes to avoiding subsequent purification stages that are common in the existing chemical processes. Finally, biocatalysts promise to prevent stream wastes, and the implemented agents consist of renewable materials [170], which are important considerations for any process, especially those related to biorefineries.

3.2. Carbon Dioxide Conversion through Heterogeneous Catalysis

Greenhouse gas (GHG) emissions constitute a current issue that demands new alternatives be implemented in the industrial sector to mitigate environmental implications. Within the total GHG emissions, CO₂ occupies the second position after methane [181], representing an increase in concentration in the atmosphere by up to 400 ppm in recent years [182]. There have been several studies where CO₂ utilization (CDU) is carried out to promote the production of high-value-added products when using catalysis [183]. Nevertheless, a complete integration of CO₂ capture and storage (CCS) systems to utilize technologies by which this gas could be transformed to different polymeric, organic, and inorganic products [184] should be analyzed.

A complete analysis of CO₂ as a raw material in transformation routes according to the production scale contributes to mitigating environmental problems. Moreover, the production of different compounds that are currently of great interest could be favored [185]. To achieve this proposal, new transformation routes in processing plants with CO₂ streams that can be used as raw material must be installed after having developed the respective sustainability assessment, where the techno-economic, environmental, and social dimensions are considered [186]. Some of the investigated methods for CO₂ conversion to chemicals include electrocatalytic or photocatalytic reduction, bio-catalysis, dry methane reforming, and catalytic hydrogenation [187]. Advances in molecular catalysis for electrocatalytic capture of CO₂ have indicated the process to be an appealing option for transformation of CO₂ to chemicals such as carbon monoxide, formic acid, formaldehyde, and ethanol [188].

Von der Assen has focused on the evaluation of producing dimethyl carbonate (DMC) by several reaction routes through the CDU concept [189]. This product is an important carbonylating compound that can be utilized for different fields including electronics, chemicals, pesticides, and medicine [190]. Two main routes that use CO₂ as raw material are the direct synthesis from CO₂ and methanol, and the synthesis from propylene carbonate, which is also known as the PC-route. Furthermore, a high-level conversion (85.2%) can be reached with a zirconium (IV) acetylacetonate (Zr(acac)₄) catalyst, leading to a carboxymethylation with a selectivity up to 99% [191]. Tamboli et al. [181] also studied the conversion of CO₂ into DMC in a batch operating mode by using methanol as raw material to obtain a product yield of 26.17 wt% when the catalyst involved is Ce_{0.5}Zr_{0.5}O₂ (see Table 8 and Figure 2). The reactions involved during the process enhance high efficiency and avoid the use of toxic chemicals such as phosgene, according to the kinetic study presented by Ohno et al. [191] and the work of Honda et al. [192].

Industrial sectors with high-residual-gas streams should consider the presented products in Table 8 to generate demanded and value-added compounds produced from CO₂ through heterogeneous catalysis, considering the great variety of products that includes fuels, chemical precursors, and medicines such as Benzamide. This compound is produced from CO₂ and low quantities of methanol when operating in high-pressure conditions to obtain a yield of 54.56 wt% [193]. Carbon monoxide (CO) can also be obtained by CO₂ reduction using Ni/nSiO₂ or Co-Fe/Al₂O₃, reaching yields up to 74 wt% with the use of the first catalyst operating at 800 °C and vacuum pressure [194].

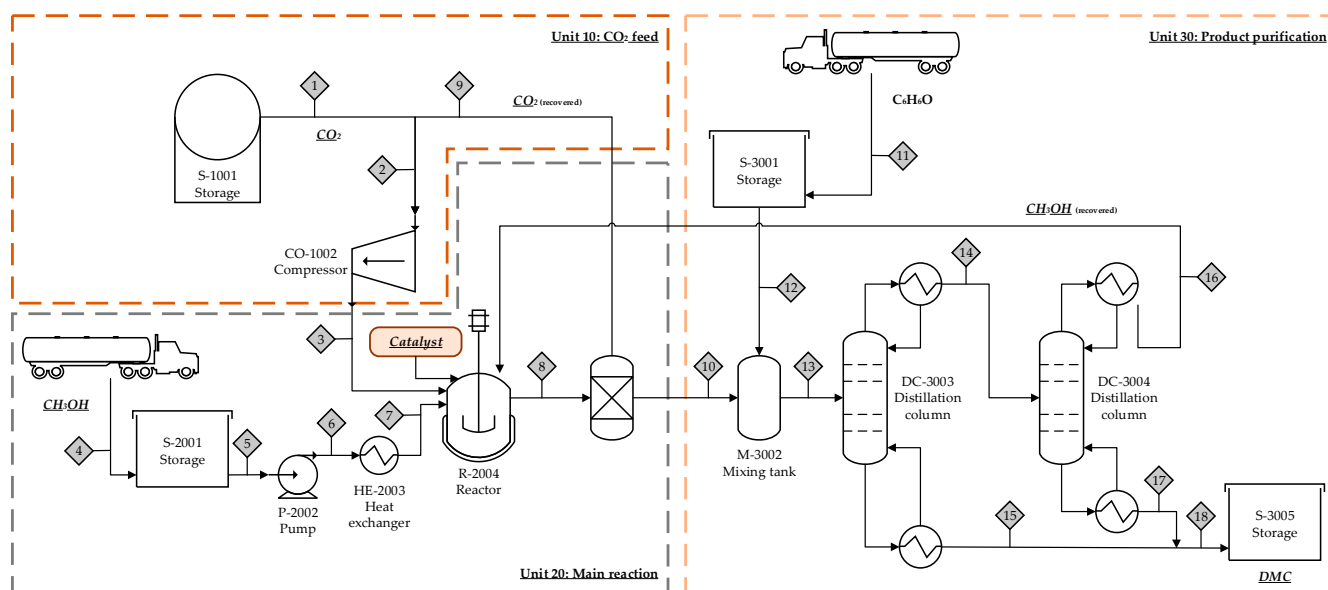


Figure 2. Schematic of the production of dimethyl carbonate (DMC) using CO_2 and methanol as raw material and $\text{Ce}_{0.5}\text{Zr}_{0.5}\text{O}_2$ as catalyst.

3.3. Catalysis Recyclability and Re-Use

Once the catalytic operation has been completed by using either a homogenous or heterogenous catalyst, the recovery of these substances implementing different technologies must be guaranteed in order to reuse them once more in the process [195]. High catalytic performance is related to ease of separation and recycling of the catalyst. When carrying out the recovery, solid loss must be minimum to enhance a techno-economic process. According to the review paper presented by Miceli et al. [196], the separation methods that include extraction, filtration, and centrifugation required more time and, consequently, there is not a real industrial application because of the high economic requirements.

Homogenous catalysts enhance important advantages when compared to heterogenous catalyst regarding the selectivity and stability [197]. Nevertheless, in terms of separation facilities forming the reactive mixture, a heterogenous catalyst is cheaper and presents a low environmental impact, as non-sophisticated technologies must be implemented. Consequently, fewer limitations are presented for heterogenous substances when considering specialty and fine chemicals obtained in, for instance, the pharmaceutical industry [198]. Moreover, for reactive mixture in gas and solid phases, the catalyst can be separated and cleaned by using conventional techniques, and as for liquid and solid systems, the catalyst matrix can be recovered by filtration [196].

As mentioned before, implementing catalyst recovery techniques guarantees economic and environmental improvements. Nevertheless, Sádaba et al. [199] explained that deactivation of the catalyst might occur by different phenomena such as poisoning, thermal degradation, or metals leaching into liquid phase. Therefore, when the recovery process has been completed several times and the catalyst activity has decreased, several authors recommend using the spent catalyst in an alternative process to mitigate environmental issues before disposition in landfills [200]. Chiranjeevi et al. [200] analyzed the minimization of spent catalyst as waste from refineries' applications and concluded that the main reasons for the recent deactivation of catalyst in oil processing include the rapid demand for product that makes the flowrates increase, the reduction in time for the operating cycles, and particular characteristics of the feedstock that cause poisoning of the catalytic substances.

Among the most used methods for catalyst recovery, filtration and centrifugation constitute the most used technologies for heterogenous substances, considering the difference in both chemical and physical properties in the reactive mixture [196]. Filtration

is carried out using a filter or membrane to remove the solid part of the liquid and gas mixture. The fluid phase that is separated from the solid fraction is called permeated, and the phenomenon is influenced by a pressure gradient. Santoro et al. [198] studied the hot filtration for the removal of solid catalyst to stop the reaction by using metal-catalyzed C-H functionalization. As for centrifugation, the driving force is the difference in density that is utilized to separate the liquid and solid mixtures. After the operation, the solid part remaining in the bottom of the flask is denominated as pellet, while the supernate refers to the fluid phase [196]. Liu et al. [201] analyzed the recovery of a silver nanoparticle catalyst by centrifugation to carry out capture and conversion of CO₂ as a low-energy-consumption alternative.

Another recycling alternative for heterogenous catalyst recovery is magnetic separation. This technique offers promising options for recycling catalyst-based metals in terms of techno-economic feasibility, as the operation takes little time and the implementation cost is low [202]. When considering a biorefinery scenario, sustainable processes must consider green chemistry principles alongside the production stages. Therefore, there might exist technologies that promote metal recovery from spent catalyst before final disposition. Miceli et al. [196] present two traditional techniques whose aim involves both economic and environmental dimensions for the production process. The first technique, denominated as hydrometallurgy, refers to metal dissolution in acid or base solution for a subsequent recovery of the specific metal by solvent extraction. Hu et al. [203] studied the removal of vanadium by ion exchange from a molybdate solution using a loaded resin that allowed a vanadium desorption ratio of 98.5% when regenerating the column. The second alternative corresponds to a pyrometallurgical process in which metal separation is carried out by using chemical treatments. Pyrolysis and incineration are involved in these treatments, which makes this process much more complex and expensive due to the high energy demand. Additionally, Peng et al. [204] mentioned that for platinum group metals recovery, vaporization techniques can be applied, but there could be corrosion as well as environmental and health impacts.

Table 8. Value-added products derived from CO₂-catalytic upgrading.

Reactants	Catalyst	Product	Operating Conditions	Reactor	Yield (wt%)	Application	Ref.
CO ₂ and methanol	Ce _{0.5} Zr _{0.5} O ₂	Dimethyl carbonate	T: 140 °C; P _{CO₂} : 7.5 MPa; R.T.: 12 h; Dehydrating agent: 2,2-Dimethoxypropane (DMP); Load: 25 mL methanol, 1 g catalyst, 1 g DMP; Stirring rate: 900 rpm.	Stainless-steel batch reactor	26.17	Green starting material for organic synthesis, solvent, and fuel.	[181]
CO ₂ and methanol	Ti _{0.10} Ce _{0.90} O ₂	Dimethyl carbonate	T: 140 °C; P: 24 bar; Methanol flow rate: 0.145 mL/min; CO ₂ flow rate: 40 mL/min. CO ₂ is initially flown for 10 min to discharge air inside the reactor.	Continuous fixed-bed reactor	19.08	Green starting material for organic synthesis, solvent, and fuel.	[189]
CO ₂ and H ₂	PdNPore (Pd/Al: 97/3 wt%)	Formic acid	T: 80 °C; P _{H₂} : 1 MPa; P _{CO₂} : 1.5 MPa; R.T.: 20 h; Load: 0.025 mmol catalyst, 3 mmol 1,8-diazabicyclo [5.4.0] undec-7-ene, and 2 mL acetonitrile; N ₂ atmosphere is required.	Autoclave reactor with a magnetic stir	86.00	Antibacterial compound. Liquid organic hydrogen carrier.	[205]
CO ₂ , H ₂ , and NaOH	Fe complex (SiMe ₃)	Sodium formate	T: 120 °C; P _{H₂} : 30 bar; P _{CO₂} : 20 bar; R.T.: 24 h; Load: 3 mmol NaOH and 0.003 mmol Fe complex; Ethanol/H ₂ O: 1.5 mL/3.0 mL.	Autoclave reactor	30.70	Production of sodium hydrosulfate and formic acid. Also used in leather and food industry.	[206]
CO ₂ and H ₂	Ni/nSiO ₂	Carbon monoxide	T: 800 °C; Vacuum pressure; H.R.: 10 °C/min; H ₂ /CO ₂ : 4/1(mol%); Load: 15 mg catalyst; Total flow rate to reactor: 100 mL/min.	Fixed-bed quartz tube reactor	74.00	Production of numerous organic and inorganic compounds.	[194]
CO ₂ and H ₂	Co-Fe/Al ₂ O ₃ (85 wt% Al ₂ O ₃)	Carbon monoxide	T: 650 °C; P: Atmospheric; R.T.: 40 h; H ₂ /CO ₂ : 3/1(mol%); Total flow rate to reactor: 230 mL/min.	Fixed-bed reactor	48.00	Production of numerous organic and inorganic compounds.	[207]
CO ₂ and H ₂	Cu ²⁺ :Zn ²⁺ :Al ³⁺ :Zr ⁴⁺ (6:3:0.5:0.5)	Methanol	T: 270 °C; P: 5 MPa; H ₂ /CO ₂ : 3/1 (mol%); Load: 1 g catalyst; Gas Hourly Space Velocity (GHSV): 4600 h ⁻¹ .	Continuous high-pressure, fixed-bed reactor	14.11	Production of plastics, paints. Also used as fuel.	[208]

Table 8. Cont.

Reactants	Catalyst	Product	Operating Conditions	Reactor	Yield (wt%)	Application	Ref.
O ₂ and H ₂	Cu/Zn/Al/Zr hydrotalcite (2:1:0.7:0.3)	Methanol	T: 230 °C; P: 5 MPa; H ₂ /CO ₂ /N ₂ : 73/24/3; Load: 0.7 g catalyst, 1.4 g quartz sand; GHSV: 8500 mL _{gcat} ⁻¹ h ⁻¹ .	Continuous fixed-bed reactor	12.30	Production of plastics, paints. Also used as fuel.	[209]
CO ₂ and polycarbonate	Ni-based catalysts	Bio-oil, biochar, and gases	T: 700 °C; H.R.: 10 °C/min; Polycarbonate particle size: <2 mm; Load: 1 g of supported catalyst; Total flow rate to reactor: 200 mL/min.	Quartz tube and external heating furnace	Bio-oil: 12.20 Biochar: 26.40 Gases: 61.40	The process allows obtaining syngas without contributing to pollutant compounds.	[210]
CO ₂ and 2-methylbut-3-yn-2-ol	Zn@RIO-1 (100 mg powder-like RIO-1)	4,4-Dimethyl-5-methylene-1,3-dioxolan-2-one (α -alkylidene cyclic carbonate)	R.T.: 10 h; P _{CO₂} : 1 atm; Load: 5 mmol 2-methylbut-3-yn-2-ol, 5 mmol DBU, 15 mg catalyst.	High-pressure stirred laboratory reactor	96.00	Polymer precursor and used for fuel and electrolytes industry.	[211]
CO ₂ and 2-methylbut-3-yn-2-ol	Zn@RIO-1 (100 mg powder-like RIO-1)	3-Cyclohexyl-5,5-dimethyl-4-methylene-oxazolidin-2-one (2-oxazolidinone)	T: 80 °C; R.T.: 10 h; P _{CO₂} : 1 atm; Load: 5 mmol 2-methylbut-3-yn-2-ol, 5 mmol cyclohexylamine, 15 mg catalyst.	High-pressure stirred laboratory reactor	92.00	For skin treatment and for infections in soft tissues.	[211]
CO ₂ , phenol, and CCl ₄	Fe ₃ O ₄ @SiO ₂ -ZnBr ₂ (15.1 wt% Zn)	Diphenyl carbonate	T: 130 °C; P _{CO₂} : 8 MPa; R.T.: 4 h; Load: 12 mmol phenol, 10 mmol CCl ₄ , 1.2 mmol catalyst; Stirring rate: 1200 rpm.	Stainless-steel reactor	28.10	Production of aromatic polycarbonates.	[212]
CO ₂ , methanol, and 2-cyanopyridine	CeO ₂	2-Picolinamide	T: 120 °C; P _{CO₂} : 5 MPa; R.T.: 10 h; Load: 100 mmol methanol, 50 mmol 2-cyanopyridine, 0.17 g catalyst.	Stainless-steel reactor	85.00	Inhibition of Poly(ADP-ribose) synthetase.	[193]
CO ₂ , methanol, and benzonitrile	CeO ₂	Benzamide	T: 120 °C; P _{CO₂} : 5 MPa; R.T.: 10 h; Load: 100 mmol methanol, 500 mmol benzonitrile, 0.17 g catalyst.	Stainless-steel autoclave reactor	54.50	Treatment of diseases related to reflux, and vomiting prevention.	[193]
CO ₂ , methanol, and H ₂	Ru ₃ (CO) ₁₂ /Rh ₂ (OAc) ₄ (Ru/Rh: 60/60 μ mol)	Acetic acid	T: 200 °C; R.T.: 12 h; CO ₂ /H ₂ : 4/4 MPa; Promoter: Lil; Ligand: Imidazole; Load: 750 μ mol ligand and 3 μ mol promoter; C.G.: Ar.	Teflon-lined stainless-steel batch reactor	77.00	Production of plastics, insecticides, rubber, and acetate derivatives.	[213]

T: Temperature. P: Pressure. P_i: Pressure of component i. R.T.: Reaction time. C.G.: Carrier gas. H.R.: Heating rate.

3.4. Biochar Use as Catalyst Source

Biochar is a carbonaceous compound derived from thermochemical processing of lignocellulosic biomass, as reviewed in previous sections. Biochar can be used to enhance soil properties, pollutant adsorption (e.g., dyes, inorganic metals, and ions), and CO₂ capture and storage. However, this material has a high potential to be used as catalyst, as physical properties such as porosity and surface area make this thermochemical product attractive [214]. In this way, biochar is a promising material to replace solid carbon-based catalysts. The most important advantages related to the use of biochar as catalysts are the low cost and easy production. Physicochemical properties of biochar can be modified using acid/base processes (e.g., impregnation).

Biochar needs to be activated to improve catalytic efficiency. Indeed, biochar properties such as surface area, porosity, pore volume, pore size, and acidity are also improved. These properties can help to increase yield, productivity, and selectivity. A way to increase biochar porosity is via hydrothermal treatment or oxygenation [215]. Examples of different reactions catalyzed by biochar are transesterification and hydrolysis. Several authors have reported biochar sulfonation using sulfuric acid and calcination. This process increases the hydrolytic capacity. Lee et al. [214] analyzed the implementation of sulfonated pine-chip biochar as catalyst for hemicellulose hydrolysis to xylose and compared the conversion obtained (85%) when applying a commercial activated carbon at similar operating conditions (see Figure 3). Another application of biochar as catalysts addresses tar cracking. Indeed, biochar can be used to increase H₂ concentration in syngas, as this compound promotes different reactions in the gasification process. Moreover, the Fisher–Tropsch reaction has been catalyzed using activated biochar. The yields obtained after the process are similar to those obtained using iron-based catalyst [216]. Finally, activated biochar can be used as acid catalyst for the lignocellulosic matrix disruption and to remove hemicellulose. Ormsby et al. [217] performed hemicellulose hydrolysis, reaching an 85% conversion to xylose. Thus, biochar can be used for producing sugar-derived compounds and chemical platforms [218].

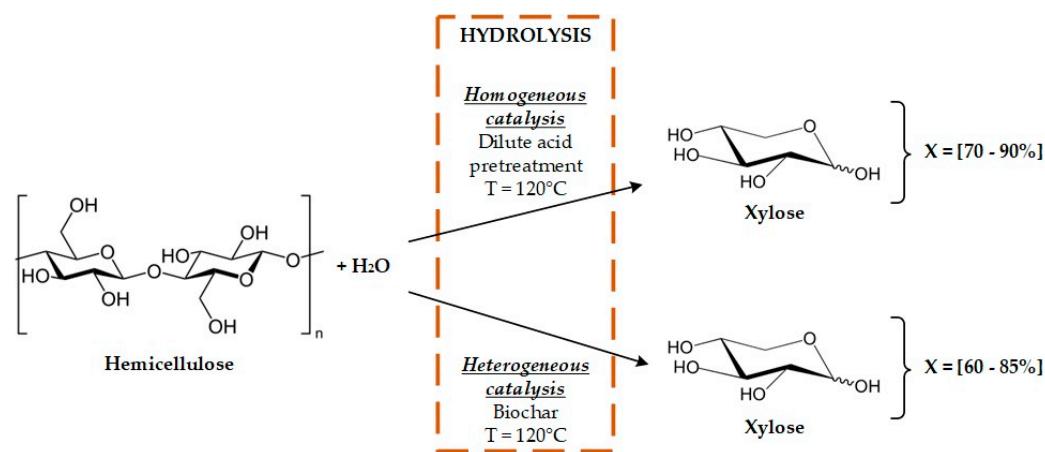


Figure 3. Implementation of biochar as catalyst for the hydrolysis of hemicellulose.

Despite the high potential of biochar to be used as catalyst, issues related to the standardized production of this material need to be researched and improved. Moreover, research on proper raw materials for biochar production is required, as the raw material chemical composition and physical properties affect the biochar quality. Another important aspect to improve biochar's use as catalyst is related to the operating conditions for producing biochar. Slow or fast pyrolysis processes should be optimized for improving the above-mentioned properties. Similar points were highlighted by Lee et al. [214]. Indeed, these authors concluded that further investigations into developing the catalytic properties of biochar are important to produce stable catalysts. If these hotspots are improved, biochar can be used as catalyst by improving the sustainability of the thermochemical production processes, as more income can be obtained from the production of biochar and other prod-

ucts (i.e., bio-oil). Furthermore, the use of biochar as catalysts also offers benefits to other processes, as biochar can be a cheaper catalyst than homogeneous (e.g., inorganic acids) or heterogeneous catalysts (e.g., zeolites).

4. Sustainability Metrics of Catalytic Biomass Upgrading in Biorefineries

Biorefineries have been defined as complex systems to upgrade biomass. These facilities aim to produce a wide range of products and energy vectors. The number of chemicals produced in a biorefinery are uncountable, as there are many pathways for biomass upgrading. Nevertheless, these possibilities can be increased by introducing catalytic processes, as catalytic conversion of biomass can increase the number of bio-based products that can be used to replace oil-based products (e.g., fuels, and polymers). Thus, conventional biorefineries involving thermochemical and biotechnological pathways can be improved with a new biorefinery system by involving catalytic and biocatalytic processes. Moreover, these new biorefineries must also perform the minimization of the environmental impact through waste-streams processing.

Future biorefineries should be sustainable. This fact implies a perfect balance between economic, environmental, and social aspects. Sustainability dimensions can be enhanced by improving technical aspects. Indeed, process conversion, yields, productivities, energy efficiency, and waste-streams flow are optimized (i.e., maximized or minimized). Figure 4 shows the role of catalytic and biocatalytic processes in future biorefineries, as these processes can be introduced into thermochemical and biotechnological routes. The design of these biorefineries must involve not only the classical definitions of the knowledge-based and optimization approaches. The design of future biorefineries must involve a comprehensive design to improve technical, economic, and environmental aspects, as studied for sustainable energy production in a soybean biorefinery by Paulinetti et al. [219]. In this research paper, the authors analyzed the implementation of anaerobic digestors on an industrial scale for the treatment of soybean molasses, resulting in different reactor configurations that represent initial investments of USD 5.8 and 7.6 million, with annual returns of USD 1 and 2.2 million, respectively.

Using lignocellulosic materials as feedstocks in biorefineries to produce value-added products has been profiled as a potential option to produce value-added products. However, biorefinery implementation is still restricted, as most biotechnological conversion pathways do not have a high Technological Readiness Level (TRL). Therefore, more efforts are needed to ease the transition from oil-based to bio-based sources. Moreover, implementing biotechnological processes can have a higher complexity level, as the microorganisms need specific growth conditions. This fact directly relates to the total capital costs associated with the technologies employed for the conversion of this raw material into liquid transportation fuels or chemicals. The second-generation feedstock biorefining comprises pretreatment, transformation/reaction, and separation/purification stages, where high-cost technologies and high energy requirements have caused a slow application of these raw materials at the industrial level. Therefore, new challenges in this area have surged to increase the possibility of using this type of feedstock.

The above-mentioned processes use substances known as catalysts, which increase the reaction rate to obtain the desired products without being consumed or modifying the reaction's chemical equilibrium. Depending on the catalyst used, catalytic processes can be classified into homogeneous and heterogeneous catalysis. The main difference between these types of catalysis is that one occurs in the liquid phase and the other in the solid phase. In addition, heterogeneous catalysis has the following advantages over homogeneous catalysis: high stability under severe temperature conditions and easy recovery and reuse.

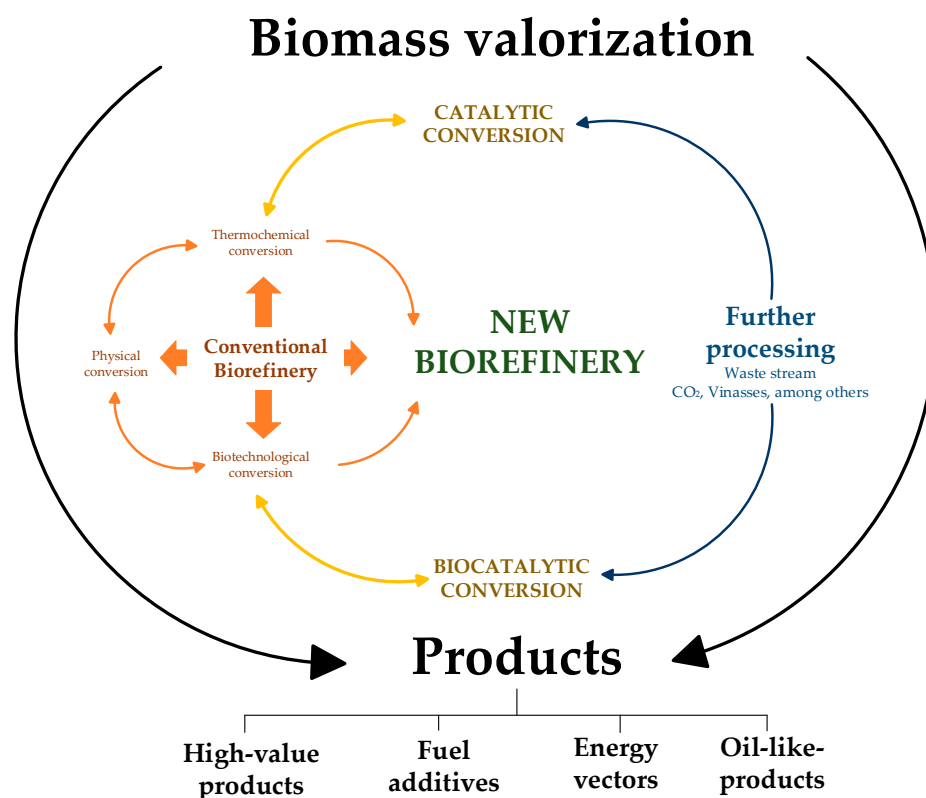


Figure 4. Integration of catalytic, biocatalytic, and waste-streams-upgrading processes into conventional biorefineries for increasing sustainability.

According to the above, implementing catalytic processes to convert the main components of lignocellulosic materials into compounds that can be applied to different sectors is an interesting alternative. In the current proposed biorefineries, homogeneous catalysis has been employed in the pretreatment stage to remove hemicellulose (xylan) through a diluted acid process and to degrade the cellulose to fermentable sugars through enzymatic hydrolysis. Nevertheless, other processes such as gasification, pyrolysis, and liquefaction have begun to be improved using heterogeneous and homogeneous catalysis. Table 9 shows the results for the technical, economic, and environmental dimensions of some biorefineries where catalysis is implemented.

The implementation of catalysis in biorefineries has not yet been studied from a complete sustainability perspective where technical, economic, environmental, and social impacts are considered. Table 9 shows that for the obtaining of high-value-added products and fuels, current sustainable metrics have mainly included technical factors regarding the catalyst performance for a determined biomass-upgrading process. Moreover, considering the aim of this study to highlight the role of the catalysis in boosting biomass use at the industrial level, the creation of a common framework is necessary for a complete analysis of future biorefineries where catalytic processes are required to establish the possibility of a real scaling.

Table 9. Sustainability metrics of biomass-upgrading processes reported in the open literature.

Raw Material	Product	Catalysis	Process Description	Sustainability Metrics			Ref.
				Technical	Economic	Environmental	
Wheat straw	Hydrogen	Straw-derived biochar	Catalytic gasification by using straw-derived biochar catalyst in a two-stage fixed-bed reactor.	Yield: 25.59 g H ₂ /kg wheat straw	N.R.	Emitted CO ₂ : 81.35 kg/kg H ₂	[220]
Biomass-derived cellulose	2,5-Furandicarboxylic acid (FDCA)	Pt/C catalyst (5 wt% Pt)	There is a two-stage catalytic conversion system: (i) dehydration of cellulose to 5-hydroxymethylfurfural (HMF), (ii) oxidation of HMF to FDCA.	Yield: 93.6 mol%	PC: \$1532 USD/ton FDCA	N.R.	[221]
Coffee cut stems or orange peel waste	Butanol, ethanol, and mixed alcohols	Hydroxyapatite	Obtained glucose from the raw materials is catalytically converted to ethanol, butanol, and mixed alcohols. The system is integrated with a cogeneration plant.	Yield _{Butanol} : 0.048 ton/ton RM. Yield _{Ethanol} : 0.032 ton/ton RM. Yield _{Mixed alcohols} : 0.044 ton/ton RM	PC _{Butanol} : \$1.570 USD/kg. PC _{Ethanol} : \$0.914 USD/kg. PC _{Mixed alcohols} : \$1.261 USD/kg. PC _{Electricity} : \$0.115 USD/kg. PM _{Butanol} : 46.48%. PM _{Ethanol} : 33.72%	GWP _{Butanol} : 0.01 PEI/kg	[222]
Oil palm rachis	Ethanol, lactic acid, ethyl levulinate, <i>n</i> -pentane, and methanol	ZSM-5, Ni/SiO ₂ -Al ₂ O ₃ , and Cu/ZnO/Al ₂ O ₃	The proposed biorefinery implements heterogeneous catalysis for the obtention of the mentioned products through fermentation and anaerobic digestion processes.	Yield _{Ethanol} : 0.226 kg/kg RM. Yield _{Lactic acid} : 0.064 kg/kg RM. Yield _{Ethyl levulinate} : 0.246 kg/kg RM. Yield _{<i>n</i>-Pentane} : 0.079 kg/kg RM. Yield _{Methanol} : 0.014 kg/kg RM	PC _{Ethanol} : %1.496 USD/kg. PC _{Lactic acid} : \$7.500 USD/kg. PC _{Ethyl levulinate} : \$1.333 USD/kg. PC _{<i>n</i>-Pentane} : \$1.400 USD/kg. PC _{Methanol} : \$0.270 USD/kg. PM _{Ethanol} : -66.22%. PM _{Lactic acid} : -72.53%. PM _{Ethyl levulinate} : 73.34%. PM _{<i>n</i>-Pentane} : 6.67%. PM _{Methanol} : 26.23%. PBP: 5 years	N.R.	[2]
Olive tree biomass	Bioethanol	Carbon-based catalyst (C-SO ₃ H)	Catalysis is implemented during the pretreatment stages of the biorefineries with a solid loading of 15 wt% in order to solubilize lignin and cellulose fractions in biomass to release fermentable sugars.	Yield: 110.83 kg/t RM	PC: \$2.55 USD/L	Emitted CO ₂ : 3287.18 kg/h	[223]

PC: Production cost. PM: Profit margin. PBP: Payback period. GWP: Global warming potential. RM: Raw material N.R.: None reported.

5. Practical Implications

Catalysis is a fundamental area with the potential to be introduced in a stronger way in current biorefineries and biomass-upgrading systems, as this area increases the number of products that can be obtained from biomass. This review can contribute to understanding some of the most recent catalytic processes applied to upgrade biomass, as well as recent trends to improve biorefineries' sustainability based on waste-streams valorization. Moreover, this review tries to give additional information about biocatalysis, CO₂ conversion, biochar use as a catalyst, and solid catalysts recyclability and re-use as a complement to other review paper in the open literature. Several research ideas can be extracted from this paper (e.g., a kinetic study of the catalytic pyrolysis and gasification, techno-economic and environmental assessment of catalysts involved in biorefineries, biochar use as a potential catalyst for hemicellulose removal, biocatalysis implementation in biorefineries). Finally, this review paper offers readers much information related to biomass catalytic conversion, considering raw materials, products, yields, operating conditions, and catalyst effect. This information can be used as the basis for proposing new experiments and scale processes.

6. Conclusions

Catalysis plays an important role in the development of new and improved biorefineries, as this area can help to increase sustainability. Thermochemical upgrading of biomass is one of the research areas that has been most studied, as gasification, pyrolysis, and hydrothermal treatment have high TRL. Thus, improving yields and conversions by adding solid catalysts provides a reliable and efficient alternative to promote biomass use instead of non-renewable resources. Indeed, catalysis is capable of reducing tar, increasing hydrocarbons, and promoting hydrogen production. On the other hand, catalysis implementation for biomass disruption and platform-molecule production is still under development. Research has been performed to study different types of catalysts. Nevertheless, few processes have a high TRL (i.e., low implementation at the industrial level). Platform molecules and high-value-added products derived from catalytic processes are being proposed as the future for increasing biorefineries' sustainability and decreasing crude-oil dependency. Catalytic processes are also being implemented for upgrading waste streams to minimize the environmental impact of biorefineries while increasing economic performance. CO₂ conversion, biochar use as catalyst, and biocatalysis inclusion are the most significant trends for improving biorefinery sustainability. Finally, the sustainability assessment of catalytic biomass-upgrading processes is scarce in the open literature. Thus, the real effect of implementing catalytic processes in biorefineries is now unknown, as pre-feasibility studies are needed to demonstrate the possible implementation of this kind of process at the industrial level.

Author Contributions: Conceptualization, J.C.S.-T., M.O.-S., P.-J.I.-G. and C.A.C.A.; formal analysis, C.A.C.A.; investigation, J.C.S.-T., M.O.-S. and P.-J.I.-G.; writing—original draft preparation, J.C.S.-T., M.O.-S. and P.-J.I.-G.; writing—review and editing, J.C.S.-T., M.O.-S., P.-J.I.-G. and C.A.C.A.; supervision, C.A.C.A.; funding acquisition, C.A.C.A. All authors have read and agreed to the published version of the manuscript.

Funding: This paper is the result of the research work developed through the project "Programa de Investigación Reconstrucción del Tejido Social en Zonas de Posconflicto en Colombia" with SIGP Code 57579 and the investigation project "Competencias empresariales y de innovación para el desarrollo económico y la inclusión productiva de las regiones afectadas por el conflicto colombiano" with SIGP Code 5807, financed by the Colombia Scientific Announcement (Contract No FP44842-213-2018). Moreover, the authors express their gratitude to the research project "Aprovechamiento y valorización sostenible de residuos sólidos orgánicos y su posible aplicación en biorrefinerías y tecnologías de residuos a energía en el departamento de Sucre" code BPIN 2020000100189.

Data Availability Statement: Not applicable.

Conflicts of Interest: The authors declare no conflict of interest.

References

1. Udemba, E.N.; Tosun, M. Energy Transition and Diversification: A Pathway to Achieve Sustainable Development Goals (SDGs) in Brazil. *Energy* **2022**, *239*, 122199. [CrossRef]
2. Cardona Alzate, C.A.; Solarte Toro, J.C.; Peña, Á.G. Fermentation, Thermochemical and Catalytic Processes in the Transformation of Biomass through Efficient Biorefineries. *Catal. Today* **2018**, *302*, 61–72. [CrossRef]
3. Wiertz, T.; Kuhn, L.; Mattissek, A. A Turn to Geopolitics: Shifts in the German Energy Transition Discourse in Light of Russia's War against Ukraine. *Energy Res. Soc. Sci.* **2023**, *98*, 103036. [CrossRef]
4. REN21 Renewables 2022 Global Status Report 2022. Available online: <https://www.ren21.net/gsr-2022/> (accessed on 30 April 2023).
5. International Energy Agency Sustainable International Bioenergy Trade: Securing Supply and Demand. Available online: http://www.fao.org/uploads/media/0611_IEA_Task_40_-_Technology_report.pdf (accessed on 1 May 2023).
6. Wang, H.; Yang, B.; Zhang, Q.; Zhu, W. Catalytic Routes for the Conversion of Lignocellulosic Biomass to Aviation Fuel Range Hydrocarbons. *Renew. Sustain. Energy Rev.* **2020**, *120*, 109612. [CrossRef]
7. Wang, J.; Liu, S.; Huang, J.; Qu, Z. A Review on Polyhydroxyalkanoate Production from Agricultural Waste Biomass: Development, Advances, Circular Approach, and Challenges. *Bioresour. Technol.* **2021**, *342*, 126008. [CrossRef]
8. Mujtaba, M.; Fraceto, L.; Fazeli, M.; Mukherjee, S.; Savassa, S.M.; de Medeiros, G.A.; do Espírito Santo Pereira, A.; Mancini, S.D.; Lipponen, J.; Vilaplana, F. Lignocellulosic Biomass from Agricultural Waste to the Circular Economy: A Review with Focus on Biofuels, Biocomposites and Bioplastics. *J. Clean. Prod.* **2023**, *402*, 136815. [CrossRef]
9. Wang, W.; Gu, Y.; Zhou, C.; Hu, C. Current Challenges and Perspectives for the Catalytic Pyrolysis of Lignocellulosic Biomass to High-Value Products. *Catalysts* **2022**, *12*, 1524. [CrossRef]
10. Aristizábal-Marulanda, V.; Solarte-Toro, J.C.; Cardona Alzate, C.A. Study of Biorefineries Based on Experimental Data: Production of Bioethanol, Biogas, Syngas, and Electricity Using Coffee-Cut Stems as Raw Material. *Environ. Sci. Pollut. Res.* **2021**, *28*, 24590–24604. [CrossRef]
11. Shen, Y. A Review on Hydrothermal Carbonization of Biomass and Plastic Wastes to Energy Products. *Biomass Bioenergy* **2020**, *134*, 105479. [CrossRef]
12. Morakile, T.; Mandegari, M.; Farzad, S.; Görgens, J.F. Comparative Techno-Economic Assessment of Sugarcane Biorefineries Producing Glutamic Acid, Levulinic Acid and Xylitol from Sugarcane. *Ind. Crops Prod.* **2022**, *184*, 115053. [CrossRef]
13. Ahorsu, R.; Constanti, M.; Medina, F. Recent Impacts of Heterogeneous Catalysis in Biorefineries. *Ind. Eng. Chem. Res.* **2021**, *60*, 18612–18626. [CrossRef]
14. Karupphasamy, K.; Theerthagiri, J.; Selvaraj, A.; Vikraman, D.; Parangusan, H.; Mythili, R.; Choi, M.Y.; Kim, H.S. Current Trends and Prospects in Catalytic Upgrading of Lignocellulosic Biomass Feedstock into Ultrapure Biofuels. *Environ. Res.* **2023**, *226*, 115660. [CrossRef]
15. Khemthong, P.; Yimsukanan, C.; Narkkun, T.; Srifa, A.; Witoon, T.; Pongchaiphol, S.; Kiatphuengporn, S.; Faungnawakij, K. Advances in Catalytic Production of Value-Added Biochemicals and Biofuels via Furfural Platform Derived Lignocellulosic Biomass. *Biomass Bioenergy* **2021**, *148*, 106033. [CrossRef]
16. Deng, F.; Amarasekara, A.S. Catalytic Upgrading of Biomass Derived Furans. *Ind. Crops Prod.* **2021**, *159*, 113055. [CrossRef]
17. Yan, P.; Wang, H.; Liao, Y.; Wang, C. Zeolite Catalysts for the Valorization of Biomass into Platform Compounds and Biochemicals/Biofuels: A Review. *Renew. Sustain. Energy Rev.* **2023**, *178*, 113219. [CrossRef]
18. Moncada, B.J.; Aristizábal, M.V.; Cardona, A.C.A. Design Strategies for Sustainable Biorefineries. *Biochem. Eng. J.* **2016**, *116*, 122–134. [CrossRef]
19. Palmeros Parada, M.; Osseweijer, P.; Posada Duque, J.A. Sustainable Biorefineries, an Analysis of Practices for Incorporating Sustainability in Biorefinery Design. *Ind. Crops Prod.* **2017**, *106*, 105–123. [CrossRef]
20. Solarte-Toro, J.C.; Cardona Alzate, C.A. Biorefineries as the Base for Accomplishing the Sustainable Development Goals (SDGs) and the Transition to Bioeconomy: Technical Aspects, Challenges and Perspectives. *Bioresour. Technol.* **2021**, *340*, 125626. [CrossRef]
21. Solarte-Toro, J.C.; Laghezza, M.; Fiore, S.; Berruti, F.; Moustakas, K.; Cardona Alzate, C.A. Review of the Impact of Socio-Economic Conditions on the Development and Implementation of Biorefineries. *Fuel* **2022**, *328*, 125169. [CrossRef]
22. Shah, A.A.; Sharma, K.; Haider, M.S.; Toor, S.S.; Rosendahl, L.A.; Pedersen, T.H.; Castello, D. The Role of Catalysts in Biomass Hydrothermal Liquefaction and Biocrude Upgrading. *Processes* **2022**, *10*, 207. [CrossRef]
23. Vamvuka, D. Bio-Oil, Solid and Gaseous Biofuels from Biomass Pyrolysis Processes—An Overview. *Int. J. Energy Res.* **2011**, *35*, 835–862. [CrossRef]
24. Solarte-Toro, J.C.; González-Aguirre, J.A.; Poveda Giraldo, J.A.; Cardona Alzate, C.A. Thermochemical Processing of Woody Biomass: A Review Focused on Energy-Driven Applications and Catalytic Upgrading. *Renew. Sustain. Energy Rev.* **2021**, *136*, 110376. [CrossRef]
25. Arnold, R.A.; Hill, J.M. Catalysts for Gasification: A Review. *Sustain. Energy Fuels* **2019**, *3*, 656–672. [CrossRef]
26. Hou, S.S.; Huang, W.C.; Lin, T.H. Co-Combustion of Fast Pyrolysis Bio-Oil Derived from Coffee Bean Residue and Diesel in an Oil-Fired Furnace. *Appl. Sci.* **2017**, *7*, 1085. [CrossRef]
27. Dickerson, T.; Soria, J. Catalytic Fast Pyrolysis: A Review. *Energies* **2013**, *6*, 514–538. [CrossRef]

28. Rahman, M.M.; Liu, R.; Cai, J. Catalytic Fast Pyrolysis of Biomass over Zeolites for High Quality Bio-Oil—A Review. *Fuel Process. Technol.* **2018**, *180*, 32–46. [[CrossRef](#)]
29. Dada, T.K.; Sheehan, M.; Murugavelh, S.; Antunes, E. A Review on Catalytic Pyrolysis for High-Quality Bio-Oil Production from Biomass. *Biomass Convers. Biorefin.* **2023**, *13*, 2595–2614. [[CrossRef](#)]
30. Li, Y.; Nishu; Yellezuome, D.; Li, C.; Liu, R. Deactivation Mechanism and Regeneration Effect of Bi-Metallic Fe-Ni/ZSM-5 Catalyst during Biomass Catalytic Pyrolysis. *Fuel* **2022**, *312*, 122924. [[CrossRef](#)]
31. Ouedraogo, A.S.; Bhoi, P.R.; Gerdmann, C.; Patil, V.; Adhikari, S. Improving Hydrocarbons and Phenols in Bio-Oil through Catalytic Pyrolysis of Pine Sawdust. *J. Energy Inst.* **2021**, *99*, 9–20. [[CrossRef](#)]
32. Wang, K.; Kim, K.H.; Brown, R.C. Catalytic Pyrolysis of Individual Components of Lignocellulosic Biomass. *Green Chem.* **2014**, *16*, 727–735. [[CrossRef](#)]
33. Wang, K.; Brown, R.C.; Homsy, S.; Martinez, L.; Sidhu, S.S. Fast Pyrolysis of Microalgae Remnants in a Fluidized Bed Reactor for Bio-Oil and Biochar Production. *Bioresour. Technol.* **2013**, *127*, 494–499. [[CrossRef](#)] [[PubMed](#)]
34. Wang, C.; Hao, Q.; Lu, D.; Jia, Q.; Li, G.; Xu, B. Production of Light Aromatic Hydrocarbons from Biomass by Catalytic Pyrolysis. *Chin. J. Catal.* **2008**, *29*, 907–912. [[CrossRef](#)]
35. Kantarelis, E.; Yang, W.; Blasiak, W. Production of Liquid Feedstock from Biomass via Steam Pyrolysis in a Fluidized Bed Reactor. *Energy Fuels* **2013**, *27*, 4748–4759. [[CrossRef](#)]
36. Kantarelis, E.; Yang, W.; Blasiak, W. Effects of Silica-Supported Nickel and Vanadium on Liquid Products of Catalytic Steam Pyrolysis of Biomass. *Energy Fuels* **2014**, *28*, 591–599. [[CrossRef](#)]
37. Gucho, E.M.; Shahzad, K.; Bramer, E.A.; Akhtar, N.A.; Brem, G. Experimental Study on Dry Torrefaction of Beech Wood and Miscanthus. *Energies* **2015**, *8*, 3903. [[CrossRef](#)]
38. Iliopoulou, E.F.; Stefanidis, S.; Kalogiannis, K.; Psarras, A.C.; Delimitis, A.; Triantafyllidis, K.S.; Lappas, A.A. Pilot-Scale Validation of Co-ZSM-5 Catalyst Performance in the Catalytic Upgrading of Biomass Pyrolysis Vapours. *Green Chem.* **2014**, *16*, 662–674. [[CrossRef](#)]
39. Hassan, E.B.; Abou-Yousef, H.; Steele, P.; El-Giar, E. Characterization of Bio-Oils from the Fast Pyrolysis of White Oak and Sweetgum. *Energy Sources Part A Recovery Util. Environ. Eff.* **2016**, *38*, 43–50. [[CrossRef](#)]
40. Mullen, C.A.; Boateng, A.A.; Mihalcik, D.J.; Goldberg, N.M. Catalytic Fast Pyrolysis of White Oak Wood in a Bubbling Fluidized Bed. *Energy Fuels* **2011**, *25*, 5444–5451. [[CrossRef](#)]
41. Rizkiana, J.; Guan, G.; Widayatno, W.B.; Hao, X.; Huang, W.; Tsutsumi, A.; Abudula, A. Effect of Biomass Type on the Performance of Cogasification of Low Rank Coal with Biomass at Relatively Low Temperatures. *Fuel* **2014**, *134*, 414–419. [[CrossRef](#)]
42. Rizkiana, J.; Guan, G.; Widayatno, W.B.; Yang, J.; Hao, X.; Matsuo, K.; Abudula, A. Mg-Modified Ultra-Stable γ Type Zeolite for the Rapid Catalytic Co-Pyrolysis of Low-Rank Coal and Biomass. *RSC Adv.* **2016**, *6*, 2096–2105. [[CrossRef](#)]
43. Zhang, S.; Zhang, H.; Liu, X.; Zhu, S.; Hu, L.; Zhang, Q. Upgrading of Bio-Oil from Catalytic Pyrolysis of Pretreated Rice Husk over Fe-Modified ZSM-5 Zeolite Catalyst. *Fuel Process. Technol.* **2018**, *175*, 17–25. [[CrossRef](#)]
44. Balasundram, V.; Ibrahim, N.; Kasmani, R.M.; Isha, R.; Hamid, M.K.A.; Hasbullah, H.; Ali, R.R. Catalytic Upgrading of Sugarcane Bagasse Pyrolysis Vapours over Rare Earth Metal (Ce) Loaded HZSM-5: Effect of Catalyst to Biomass Ratio on the Organic Compounds in Pyrolysis Oil. *Appl. Energy* **2018**, *220*, 787–799. [[CrossRef](#)]
45. Nanda, S.; Reddy, S.N.; Vo, D.V.N.; Sahoo, B.N.; Kozinski, J.A. Catalytic Gasification of Wheat Straw in Hot Compressed (Subcritical and Supercritical) Water for Hydrogen Production. *Energy Sci. Eng.* **2018**, *6*, 448–459. [[CrossRef](#)]
46. Krishna, B.B.; Singh, R.; Bhaskar, T. Effect of Catalyst Contact on the Pyrolysis of Wheat Straw and Wheat Husk. *Fuel* **2015**, *160*, 64–70. [[CrossRef](#)]
47. Javed, S.H.; Aslam, U.; Kazmi, M.; Rustam, M.; Riaz, S.; Munir, Z. Studies on Thermal Degradation Behavior of Siliceous Agriculture Waste (Rice Husk, Wheat Husk and Bagasse). *Pol. J. Chem. Technol.* **2015**, *17*, 47–51. [[CrossRef](#)]
48. Kim, Y.M.; Jae, J.; Lee, H.W.; Han, T.U.; Lee, H.; Park, S.H.; Kim, S.; Watanabe, C.; Park, Y.K. Ex-Situ Catalytic Pyrolysis of Citrus Fruit Peels over Mesoporous MFI and Al-MCM-41. *Energy Convers. Manag.* **2016**, *125*, 277–289. [[CrossRef](#)]
49. Mohamed, B.A.; Ellis, N.; Kim, C.S.; Bi, X. Microwave-Assisted Catalytic Biomass Pyrolysis: Effects of Catalyst Mixtures. *Appl. Catal. B* **2019**, *253*, 226–234. [[CrossRef](#)]
50. Mohamed, B.A.; Ellis, N.; Kim, C.S.; Bi, X. Understanding Catalytic Effects of Bentonite/Clinoptilolite on Biomass Pyrolysis. *Renew. Energy* **2019**, *142*, 304–315. [[CrossRef](#)]
51. Chen, X.; Chen, Y.; Yang, H.; Wang, X.; Che, Q.; Chen, W.; Chen, H. Catalytic Fast Pyrolysis of Biomass: Selective Deoxygenation to Balance the Quality and Yield of Bio-Oil. *Bioresour. Technol.* **2019**, *273*, 153–158. [[CrossRef](#)]
52. Ratnasari, D.K.; Bijl, A.; Yang, W.; Jönsson, P.G. Effect of H-ZSM-5 and Al-MCM-41 Proportions in Catalyst Mixtures on the Composition of Bio-Oil in Ex-Situ Catalytic Pyrolysis of Lignocellulose Biomass. *Catalysts* **2020**, *10*, 868. [[CrossRef](#)]
53. Humbird, D.; Trendewicz, A.; Braun, R.; Dutta, A. One-Dimensional Biomass Fast Pyrolysis Model with Reaction Kinetics Integrated in an Aspen Plus Biorefinery Process Model. *ACS Sustain. Chem. Eng.* **2017**, *5*, 2463–2470. [[CrossRef](#)]
54. Safarian, S.; Rydén, M.; Janssen, M. Development and Comparison of Thermodynamic Equilibrium and Kinetic Approaches for Biomass Pyrolysis Modeling. *Energies* **2022**, *15*, 3999. [[CrossRef](#)]
55. Brown, R.C. *Thermochemical Processing of Biomass: Conversion into Fuels, Chemicals and Power*; John Wiley and Sons: Hoboken, NJ, USA, 2011; ISBN 9780470721117.

56. Solarte-Toro, J.C.; Chacón-Pérez, Y.; Cardona-Alzate, C.A. Evaluation of Biogas and Syngas as Energy Vectors for Heat and Power Generation Using Lignocellulosic Biomass as Raw Material. *Electron. J. Biotechnol.* **2018**, *33*, 52–62. [\[CrossRef\]](#)
57. Tezer, Ö.; Karabağ, N.; Öngen, A.; Çolpan, C.Ö.; Ayol, A. Biomass Gasification for Sustainable Energy Production: A Review. *Int. J. Hydrogen Energy* **2022**, *47*, 15419–15433. [\[CrossRef\]](#)
58. Ghodke, P.K.; Sharma, A.K.; Jayaseelan, A.; Gopinath, K.P. Hydrogen-Rich Syngas Production from the Lignocellulosic Biomass by Catalytic Gasification: A State of Art Review on Advance Technologies, Economic Challenges, and Future Prospectus. *Fuel* **2023**, *342*, 127800. [\[CrossRef\]](#)
59. Veses, A.; Aznar, M.; López, J.M.; Callén, M.S.; Murillo, R.; García, T. Production of Upgraded Bio-Oils by Biomass Catalytic Pyrolysis in an Auger Reactor Using Low Cost Materials. *Fuel* **2015**, *141*, 17–22. [\[CrossRef\]](#)
60. Aysu, T. Catalytic Pyrolysis of Eremurus Spectabilis for Bio-Oil Production in a Fixed-Bed Reactor: Effects of Pyrolysis Parameters on Product Yields and Character. *Fuel Process. Technol.* **2015**, *129*, 24–38. [\[CrossRef\]](#)
61. Veses, A.; Aznar, M.; Martínez, I.; Martínez, J.D.; López, J.M.; Navarro, M.V.; Callén, M.S.; Murillo, R.; García, T. Catalytic Pyrolysis of Wood Biomass in an Auger Reactor Using Calcium-Based Catalysts. *Bioresour. Technol.* **2014**, *162*, 250–258. [\[CrossRef\]](#)
62. Maisano, S.; Urbani, F.; Mondello, N.; Chiodo, V. Catalytic Pyrolysis of Mediterranean Sea Plant for Bio-Oil Production. *Int. J. Hydrogen Energy* **2017**, *42*, 28082–28092. [\[CrossRef\]](#)
63. Aysu, T.; Durak, H.; Güner, S.; Bengü, A.Ş.; Esim, N. Bio-Oil Production via Catalytic Pyrolysis of Anchusa Azurea: Effects of Operating Conditions on Product Yields and Chromatographic Characterization. *Bioresour. Technol.* **2016**, *205*, 7–14. [\[CrossRef\]](#)
64. Song, H.; Yang, G.; Xue, P.; Li, Y.; Zou, J.; Wang, S.; Yang, H.; Chen, H. Recent Development of Biomass Gasification for H₂ Rich Gas Production. *Appl. Energy Combust. Sci.* **2022**, *10*, 100059. [\[CrossRef\]](#)
65. dos Santos, R.G.; Alencar, A.C. Biomass-Derived Syngas Production via Gasification Process and Its Catalytic Conversion into Fuels by Fischer Tropsch Synthesis: A Review. *Int. J. Hydrogen Energy* **2020**, *45*, 18114–18132. [\[CrossRef\]](#)
66. Poto, S.; Vico van Berkel, D.; Gallucci, F.; Fernanda Neira d’Angelo, M. Kinetic Modelling of the Methanol Synthesis from CO₂ and H₂ over a CuO/CeO₂/ZrO₂ Catalyst: The Role of CO₂ and CO Hydrogenation. *Chem. Eng. J.* **2022**, *435*, 134946. [\[CrossRef\]](#)
67. Zhang, W.; Wu, Y.; Huang, S.; Wei, X.; Li, X.; Wu, S. Comparative Study on the Effects of Wood Dust and Rice Husk on Wheat Straw Gasification Process: Ash Fusion Characteristics and Gasification Reactivity. *Fuel* **2022**, *326*, 124942. [\[CrossRef\]](#)
68. Lv, P.; Yuan, Z.; Wu, C.; Ma, L.; Chen, Y.; Tsubaki, N. Bio-Syngas Production from Biomass Catalytic Gasification. *Energy Convers. Manag.* **2007**, *48*, 1132–1139. [\[CrossRef\]](#)
69. Jin, F.; Sun, H.; Wu, C.; Ling, H.; Jiang, Y.; Williams, P.T.; Huang, J. Effect of Calcium Addition on Mg-AlO_x Supported Ni Catalysts for Hydrogen Production from Pyrolysis-Gasification of Biomass. *Catal. Today* **2018**, *309*, 2–10. [\[CrossRef\]](#)
70. Wu, C.; Wang, L.; Williams, P.T.; Shi, J.; Huang, J. Hydrogen Production from Biomass Gasification with Ni/MCM-41 Catalysts: Influence of Ni Content. *Appl. Catal. B* **2011**, *108–109*, 6–13. [\[CrossRef\]](#)
71. Cao, J.P.; Shi, P.; Zhao, X.Y.; Wei, X.Y.; Takarada, T. Decomposition of NO_x Precursors during Gasification of Wet and Dried Pig Manures and Their Composts over Ni-Based Catalysts. *Energy Fuels* **2014**, *28*, 2041–2046. [\[CrossRef\]](#)
72. Li, W.; Ren, J.; Zhao, X.Y.; Takarada, T. H₂ and Syngas Production from Catalytic Cracking of Pig Manure and Compost Pyrolysis Vapor over Ni-Based Catalysts. *Pol. J. Chem. Technol.* **2018**, *20*, 8–14. [\[CrossRef\]](#)
73. Cao, J.P.; Huang, X.; Zhao, X.Y.; Wang, B.S.; Meesuk, S.; Sato, K.; Wei, X.Y.; Takarada, T. Low-Temperature Catalytic Gasification of Sewage Sludge-Derived Volatiles to Produce Clean H₂-Rich Syngas over a Nickel Loaded on Lignite Char. *Int. J. Hydrogen Energy* **2014**, *39*, 9193–9199. [\[CrossRef\]](#)
74. Wang, B.S.; Cao, J.P.; Zhao, X.Y.; Bian, Y.; Song, C.; Zhao, Y.P.; Fan, X.; Wei, X.Y.; Takarada, T. Preparation of Nickel-Loaded on Lignite Char for Catalytic Gasification of Biomass. *Fuel Process. Technol.* **2015**, *136*, 17–24. [\[CrossRef\]](#)
75. Cao, J.P.; Liu, T.L.; Ren, J.; Zhao, X.Y.; Wu, Y.; Wang, J.X.; Ren, X.Y.; Wei, X.Y. Preparation and Characterization of Nickel Loaded on Resin Char as Tar Reforming Catalyst for Biomass Gasification. *J. Anal. Appl. Pyrolysis* **2017**, *127*, 82–90. [\[CrossRef\]](#)
76. Rapagná, S.; Provendier, H.; Petit, C.; Kiennemann, A.; Foscolo, P.U. Development of Catalysts Suitable for Hydrogen or Syn-Gas Production from Biomass Gasification. *Biomass Bioenergy* **2002**, *22*, 377–388. [\[CrossRef\]](#)
77. Cao, W.; Guo, L.; Yan, X.; Zhang, D.; Yao, X. Assessment of Sugarcane Bagasse Gasification in Supercritical Water for Hydrogen Production. *Int. J. Hydrogen Energy* **2018**, *43*, 13711–13719. [\[CrossRef\]](#)
78. Sahoo, A.; Ram, D.K. Gasifier Performance and Energy Analysis for Fluidized Bed Gasification of Sugarcane Bagasse. *Energy* **2015**, *90*, 1420–1425. [\[CrossRef\]](#)
79. Zhang, G.; Liu, H.; Wang, J.; Wu, B. Catalytic Gasification Characteristics of Rice Husk with Calcined Dolomite. *Energy* **2018**, *165*, 1173–1177. [\[CrossRef\]](#)
80. Hamad, M.A.; Radwan, A.M.; Heggo, D.A.; Moustafa, T. Hydrogen Rich Gas Production from Catalytic Gasification of Biomass. *Renew. Energy* **2016**, *85*, 1290–1300. [\[CrossRef\]](#)
81. Wang, T.; Zhai, Y.; Zhu, Y.; Li, C.; Zeng, G. A Review of the Hydrothermal Carbonization of Biomass Waste for Hydrochar Formation: Process Conditions, Fundamentals, and Physicochemical Properties. *Renew. Sustain. Energy Rev.* **2018**, *90*, 223–247. [\[CrossRef\]](#)
82. Djandja, O.S.; Liew, R.K.; Liu, C.; Liang, J.; Yuan, H.; He, W.; Feng, Y.; Lougou, B.G.; Duan, P.G.; Lu, X.; et al. Catalytic Hydrothermal Carbonization of Wet Organic Solid Waste: A Review. *Sci. Total Environ.* **2023**, *873*, 162119. [\[CrossRef\]](#) [\[PubMed\]](#)
83. Volpe, M.; Luz, F.C.; Saha, N.; Reza, M.T.; Mosonik, M.C.; Volpe, R.; Messineo, A. Enhancement of Energy and Combustion Properties of Hydrochar via Citric Acid Catalysed Secondary Char Production. *Biomass Convers. Biorefin.* **2021**, *1*, 1–12. [\[CrossRef\]](#)

84. Ameen, M.; Zamri, N.M.; May, S.T.; Azizan, M.T.; Aqsha, A.; Sabzoi, N.; Sher, F. Effect of Acid Catalysts on Hydrothermal Carbonization of Malaysian Oil Palm Residues (Leaves, Fronds, and Shells) for Hydrochar Production. *Biomass Convers. Biorefin.* **2022**, *12*, 103–114. [[CrossRef](#)]
85. Rather, M.A.; Khan, N.S.; Gupta, R. Catalytic Hydrothermal Carbonization of Invasive Macrophyte Hornwort (*Ceratophyllum demersum*) for Production of Hydrochar: A Potential Biofuel. *Int. J. Environ. Sci. Technol.* **2017**, *14*, 1243–1252. [[CrossRef](#)]
86. Wang, Q.; Wu, S.; Cui, D.; Zhou, H.; Wu, D.; Pan, S.; Xu, F.; Wang, Z. Co-Hydrothermal Carbonization of Organic Solid Wastes to Hydrochar as Potential Fuel: A Review. *Sci. Total Environ.* **2022**, *850*, 158034. [[CrossRef](#)]
87. Liu, Z.; Xu, Z.; Xu, L.; Buyong, F.; Chay, T.C.; Li, Z.; Cai, Y.; Hu, B.; Zhu, Y.; Wang, X. Modified Biochar: Synthesis and Mechanism for Removal of Environmental Heavy Metals. *Carbon Res.* **2022**, *1*, 8. [[CrossRef](#)]
88. Chen, H.; Gao, Y.; Li, J.; Fang, Z.; Bolan, N.; Bhatnagar, A.; Gao, B.; Hou, D.; Wang, S.; Song, H.; et al. Engineered Biochar for Environmental Decontamination in Aquatic and Soil Systems: A Review. *Carbon Res.* **2022**, *1*, 4. [[CrossRef](#)]
89. Akbari, M.; Oyedun, A.O.; Kumar, A. Comparative Energy and Techno-Economic Analyses of Two Different Configurations for Hydrothermal Carbonization of Yard Waste. *Bioresour. Technol. Rep.* **2019**, *7*, 100210. [[CrossRef](#)]
90. Hussin, F.; Hazani, N.N.; Khalil, M.; Aroua, M.K. Environmental Life Cycle Assessment of Biomass Conversion Using Hydrothermal Technology: A Review. *Fuel Process. Technol.* **2023**, *246*, 107747. [[CrossRef](#)]
91. Kabenge, I.; Omulo, G.; Banadda, N.; Seay, J.; Zziwa, A.; Kiggundu, N. Characterization of Banana Peels Wastes as Potential Slow Pyrolysis Feedstock. *J. Sustain. Dev.* **2018**, *11*. [[CrossRef](#)]
92. Zhou, N.; Chen, H.; Feng, Q.; Yao, D.; Chen, H.; Wang, H.; Zhou, Z.; Li, H.; Tian, Y.; Lu, X. Effect of Phosphoric Acid on the Surface Properties and Pb(II) Adsorption Mechanisms of Hydrochars Prepared from Fresh Banana Peels. *J. Clean. Prod.* **2017**, *165*, 221–230. [[CrossRef](#)]
93. McKendry, P. Energy Production from Biomass (Part 1): Overview of Biomass. *Bioresour. Technol.* **2002**, *83*, 37–46. [[CrossRef](#)]
94. Reza, M.T.; Rottler, E.; Herklotz, L.; Wirth, B. Hydrothermal Carbonization (HTC) of Wheat Straw: Influence of Feedwater PH Prepared by Acetic Acid and Potassium Hydroxide. *Bioresour. Technol.* **2015**, *182*, 336–344. [[CrossRef](#)]
95. Wang, Y.J.; Kang, K.; Yao, Z.L.; Sun, G.T.; Qiu, L.; Zhao, L.X.; Wang, G. Effects of Different Heating Patterns on the Decomposition Behavior of White Pine Wood during Slow Pyrolysis. *Int. J. Agric. Biol. Eng.* **2018**, *11*, 218–223. [[CrossRef](#)]
96. Ghaziaskar, A.; McRae, G.A.; MacKintosh, A.; Basu, O.D. Catalyzed Hydrothermal Carbonization with Process Liquid Recycling. *Energy Fuels* **2019**, *33*, 1167–1174. [[CrossRef](#)]
97. Simsir, H.; Eltugral, N.; Karagoz, S. Effects of Acidic and Alkaline Metal Triflates on the Hydrothermal Carbonization of Glucose and Cellulose. *Energy Fuels* **2019**, *33*, 7473–7479. [[CrossRef](#)]
98. Gu, L.; Li, B.; Wen, H.; Zhang, X.; Wang, L.; Ye, J. Co-Hydrothermal Treatment of Fallen Leaves with Iron Sludge to Prepare Magnetic Iron Product and Solid Fuel. *Bioresour. Technol.* **2018**, *257*, 229–237. [[CrossRef](#)]
99. Xu, Z.-X.; Tan, Y.; Ma, X.-Q.; Wu, S.-Y.; Zhang, B. The Influence of NaCl during Hydrothermal Carbonization for Rice Husk on Hydrochar Physicochemical Properties. *Energy* **2023**, *266*, 126463. [[CrossRef](#)]
100. Jais, F.M.; Ibrahim, S.; Chee, C.Y.; Ismail, Z. High Removal of Crystal Violet Dye and Tetracycline by Hydrochloric Acid Assisted Hydrothermal Carbonization of Sugarcane Bagasse Prepared at High Yield. *Sustain. Chem. Pharm.* **2021**, *24*, 100541. [[CrossRef](#)]
101. Koottatep, T.; Fakkaew, K.; Tajai, N.; Pradeep, S.V.; Polprasert, C. Sludge Stabilization and Energy Recovery by Hydrothermal Carbonization Process. *Renew. Energy* **2016**, *99*, 978–985. [[CrossRef](#)]
102. Qi, R.; Xu, Z.; Zhou, Y.; Zhang, D.; Sun, Z.; Chen, W.; Xiong, M. Clean Solid Fuel Produced from Cotton Textiles Waste through Hydrothermal Carbonization with FeCl₃: Upgrading the Fuel Quality and Combustion Characteristics. *Energy* **2021**, *214*, 118926. [[CrossRef](#)]
103. Tran, L.T.; Nguyen, M.Q.; Hoang, H.T.; Nguyen, H.T.; Vu, T.H.T. Catalytic Hydrothermal Carbonization of Avocado Peel. *J. Chem.* **2022**, *2022*, 5766269. [[CrossRef](#)]
104. Dedes, G.; Karnaouri, A.; Topakas, E. Novel Routes in Transformation of Lignocellulosic Biomass to Furan Platform Chemicals: From Pretreatment to Enzyme Catalysis. *Catalysts* **2020**, *10*, 743. [[CrossRef](#)]
105. Bielski, R.; Gryniewicz, G. Furan Platform Chemicals beyond Fuels and Plastics. *Green Chem.* **2021**, *23*, 7458–7487. [[CrossRef](#)]
106. Karnaouri, A.; Kalogiannis, K.G.; Staikos, S.; Karakoulia, S.; Lappas, A.A.; Topakas, E. Pretreatment of Beechwood with Polyoxometalate-Based Catalysts towards the Production of Polyunsaturated Fatty Acids by *Cryptocodium cohni*. *Ind. Crops Prod.* **2023**, *197*, 116646. [[CrossRef](#)]
107. Stoffel, R.B.; Neves, P.V.; Felissia, F.E.; Ramos, L.P.; Gassa, L.M.; Area, M.C. Hemicellulose Extraction from Slash Pine Sawdust by Steam Explosion with Sulfuric Acid. *Biomass Bioenergy* **2017**, *107*, 93–101. [[CrossRef](#)]
108. Chen, X.; Zhang, Y.; Mei, J.; Zhao, G.; Lyu, Q.; Lyu, X.; Lyu, H.; Han, L.; Xiao, W. Ball Milling for Cellulose Depolymerization and Alcoholysis to Produce Methyl Levulinate at Mild Temperature. *Fuel Process. Technol.* **2019**, *188*, 129–136. [[CrossRef](#)]
109. Yan, L.; Ma, R.; Wei, H.; Li, L.; Zou, B.; Xu, Y. Ruthenium Trichloride Catalyzed Conversion of Cellulose into 5-Hydroxymethylfurfural in Biphasic System. *Bioresour. Technol.* **2019**, *279*, 84–91. [[CrossRef](#)]
110. Moodley, P.; Kana, E.B.G. Microwave-Assisted Inorganic Salt Pretreatment of Sugarcane Leaf Waste: Effect on Physicochemical Structure and Enzymatic Saccharification. *Bioresour. Technol.* **2017**, *235*, 35–42. [[CrossRef](#)]
111. Yu, I.K.M.; Tsang, D.C.W.; Yip, A.C.K.; Chen, S.S.; Ok, Y.S.; Poon, C.S. Valorization of Food Waste into Hydroxymethylfurfural: Dual Role of Metal Ions in Successive Conversion Steps. *Bioresour. Technol.* **2016**, *219*, 338–347. [[CrossRef](#)]

112. Wiredu, B.; Amarasekara, A.S. The Effect of Metal Ions as Co-Catalysts on Acidic Ionic Liquid Catalyzed Single-Step Saccharification of Corn Stover in Water. *Bioresour. Technol.* **2015**, *189*, 405–408. [[CrossRef](#)]
113. Yang, X.; Zhao, J.; Liang, J.; Zhu, J. Efficient and Selective Catalytic Conversion of Hemicellulose in Rice Straw by Metal Catalyst under Mild Conditions. *Sustainability* **2020**, *12*, 10601. [[CrossRef](#)]
114. Guo, X.; Shu, S.; Zhang, W.; Wang, E.; Hao, J. Synergetic Degradation of Corn Cob with Inorganic Salt (or Hydrogen Peroxide) and Electron Beam Irradiation. *ACS Sustain. Chem. Eng.* **2016**, *4*, 1099–1105. [[CrossRef](#)]
115. Wang, W.; Ren, J.; Li, H.; Deng, A.; Sun, R. Direct Transformation of Xylan-Type Hemicelluloses to Furfural via SnCl₄ Catalysts in Aqueous and Biphasic Systems. *Bioresour. Technol.* **2015**, *183*, 188–194. [[CrossRef](#)] [[PubMed](#)]
116. Brazdauskas, P.; Paze, A.; Rizhikovs, J.; Puke, M.; Meile, K.; Vedernikovs, N.; Tupciauskas, R.; Andzs, M. Effect of Aluminium Sulphate-Catalysed Hydrolysis Process on Furfural Yield and Cellulose Degradation of *Cannabis sativa* L. Shives. *Biomass Bioenergy* **2016**, *89*, 98–104. [[CrossRef](#)]
117. Zhang, B.; Shahbazi, A.; Wang, L.; Whitmore, A. Effect of Magnesium Chloride on Fractionation and Enzymatic Digestibility of Cattails. *Energy Sources Part A Recovery Util. Environ. Eff.* **2016**, *38*, 1–7. [[CrossRef](#)]
118. Wang, S.; Gao, W.; Li, H.; Xiao, L.P.; Sun, R.C.; Song, G. Selective Fragmentation of Biorefinery Corncob Lignin into P-Hydroxycinnamic Esters with a Supported Zinc Molybdate Catalyst. *ChemSusChem* **2018**, *11*, 2114–2123. [[CrossRef](#)] [[PubMed](#)]
119. Zhai, Y.; Li, C.; Xu, G.; Ma, Y.; Liu, X.; Zhang, Y. Depolymerization of Lignin: Via a Non-Precious Ni-Fe Alloy Catalyst Supported on Activated Carbon. *Green Chem.* **2017**, *19*, 1895–1903. [[CrossRef](#)]
120. Ma, H.; Li, H.; Zhao, W.; Li, L.; Liu, S.; Long, J.; Li, X. Selective Depolymerization of Lignin Catalyzed by Nickel Supported on Zirconium Phosphate. *Green Chem.* **2019**, *21*, 658–668. [[CrossRef](#)]
121. Liu, X.; Bouxin, F.P.; Fan, J.; Budarin, V.L.; Hu, C.; Clark, J.H. Recent Advances in the Catalytic Depolymerization of Lignin towards Phenolic Chemicals: A Review. *ChemSusChem* **2020**, *13*, 4296–4317. [[CrossRef](#)]
122. Constant, S.; Basset, C.; Dumas, C.; Di Renzo, F.; Robitzer, M.; Barakat, A.; Quignard, F. Reactive Organosolv Lignin Extraction from Wheat Straw: Influence of Lewis Acid Catalysts on Structural and Chemical Properties of Lignins. *Ind. Crops Prod.* **2015**, *65*, 180–189. [[CrossRef](#)]
123. Jiang, Z.; Zeng, Y.; Hu, D.; Guo, R.; Yan, K.; Luque, R. Chemical Transformations of 5-Hydroxymethylfurfural into Highly Added Value Products: Present and Future. *Green Chem.* **2022**, *25*, 871–892. [[CrossRef](#)]
124. Yang, X.; Yang, L.; Fan, W.; Lin, H. Effect of Redox Properties of LaCoO₃ Perovskite Catalyst on Production of Lactic Acid from Cellulosic Biomass. *Catal. Today* **2016**, *269*, 56–64. [[CrossRef](#)]
125. Li, Z.; Wu, P.; Pang, J.; Li, X.; Zhai, S.; Zheng, M. Catalytic Conversion of Sugars into Lactic Acid via a RuOx/MoS₂ Catalyst. *Catalysts* **2023**, *13*, 545. [[CrossRef](#)]
126. Chandel, A.K.; Segato, F. *Production of Top 12 Biochemicals Selected by USDOE from Renewable Resources: Status and Innovation*; Elsevier: Amsterdam, The Netherlands, 2022.
127. Jaswal, A.; Singh, P.P.; Mondal, T. Furfural—a Versatile, Biomass-Derived Platform Chemical for the Production of Renewable Chemicals. *Green Chem.* **2022**, *24*, 510–551. [[CrossRef](#)]
128. Sinisi, A.; Degli Esposti, M.; Braccini, S.; Chiellini, F.; Guzman-Puyol, S.; Heredia-Guerrero, J.A.; Morselli, D.; Fabbri, P. Levulinic Acid-Based Bioplasticizers: A Facile Approach to Enhance the Thermal and Mechanical Properties of Polyhydroxyalkanoates. *Mater. Adv.* **2021**, *2*, 7869–7880. [[CrossRef](#)]
129. Védrine, J.C. Metal Oxides in Heterogeneous Oxidation Catalysis: State of the Art and Challenges for a More Sustainable World. *ChemSusChem* **2019**, *12*, 577–588. [[CrossRef](#)] [[PubMed](#)]
130. Rueda-Duran, C.A.; Ortiz-Sanchez, M.; Cardona-Alzate, C.A. Detailed Economic Assessment of Polylactic Acid Production by Using Glucose Platform: Sugarcane Bagasse, Coffee Cut Stems, and Plantain Peels as Possible Raw Materials. *Biomass Convers. Biorefin.* **2022**, *12*, 4419–4434. [[CrossRef](#)]
131. Chang, F.; Zhou, Q.; Pan, S.X.; He, Y. Catalytic Upgrading of Glycerol, a Promising Biodiesel Coproduct. In *Biomass, Biofuels, Biochemicals: Recent Advances in Development of Platform Chemicals*; Elsevier: Amsterdam, The Netherlands, 2019.
132. Pipitone, G.; Zoppi, G.; Pirone, R.; Bensaid, S. A Critical Review on Catalyst Design for Aqueous Phase Reforming. *Int. J. Hydrogen Energy* **2022**, *47*, 151–180. [[CrossRef](#)]
133. Morales-Marín, A.; Ayastuy, J.L.; Iriarte-Velasco, U.; Gutiérrez-Ortiz, M.A. Nickel Aluminate Spinel-Derived Catalysts for the Aqueous Phase Reforming of Glycerol: Effect of Reduction Temperature. *Appl. Catal. B* **2019**, *244*, 931–945. [[CrossRef](#)]
134. Li, X.; Zhang, L.; Wang, S.; Wu, Y. Recent Advances in Aqueous-Phase Catalytic Conversions of Biomass Platform Chemicals Over Heterogeneous Catalysts. *Front. Chem.* **2020**, *7*, 948. [[CrossRef](#)]
135. Tuck, C.O.; Pérez, E.; Horváth, I.T.; Sheldon, R.A.; Poliakoff, M. Valorization of Biomass: Deriving More Value from Waste. *Science* **2012**, *337*, 695–699. [[CrossRef](#)]
136. Wicker, R.J.; Kumar, G.; Khan, E.; Bhatnagar, A. Emergent Green Technologies for Cost-Effective Valorization of Microalgal Biomass to Renewable Fuel Products under a Biorefinery Scheme. *Chem. Eng. J.* **2021**, *415*, 128932. [[CrossRef](#)]
137. Zoppi, G.; Pipitone, G.; Pirone, R.; Bensaid, S. Aqueous Phase Reforming Process for the Valorization of Wastewater Streams: Application to Different Industrial Scenarios. *Catal. Today* **2022**, *387*, 224–236. [[CrossRef](#)]
138. Manara, P.; Zabaniotou, A. Co-Valorization of Crude Glycerol Waste Streams with Conventional and/or Renewable Fuels for Power Generation and Industrial Symbiosis Perspectives. *Waste Biomass Valorization* **2016**, *7*, 135–150. [[CrossRef](#)]

139. Chen, M.Y.; Chen, C.B.; Zada, B.; Fu, Y. Perovskite Type Oxide-Supported Ni Catalysts for the Production of 2,5-Dimethylfuran from Biomass-Derived 5-Hydroxymethylfurfural. *Green Chem.* **2016**, *18*, 3858–3866. [[CrossRef](#)]
140. Manikandan, M.; Venugopal, A.K.; Prabu, K.; Jha, R.K.; Thirumalaiswamy, R. Role of Surface Synergistic Effect on the Performance of Ni-Based Hydrotalcite Catalyst for Highly Efficient Hydrogenation of Furfural. *J. Mol. Catal. A Chem.* **2016**, *417*, 153–162. [[CrossRef](#)]
141. Chatterjee, M.; Ishizaka, T.; Kawanami, H. Selective Hydrogenation of 5-Hydroxymethylfurfural to 2,5-Bis-(Hydroxymethyl)Furan Using Pt/MCM-41 in an Aqueous Medium: A Simple Approach. *Green Chem.* **2014**, *16*, 4734–4739. [[CrossRef](#)]
142. Xiao, B.; Zheng, M.; Li, X.; Pang, J.; Sun, R.; Wang, H.; Pang, X.; Wang, A.; Wang, X.; Zhang, T. Synthesis of 1,6-Hexanediol from HMF over Double-Layered Catalysts of Pd/SiO₂ + Ir-ReOx/SiO₂ in a Fixed-Bed Reactor. *Green Chem.* **2016**, *18*, 2175–2184. [[CrossRef](#)]
143. Mei, N.; Liu, B.; Zheng, J.; Lv, K.; Tang, D.; Zhang, Z. A Novel Magnetic Palladium Catalyst for the Mild Aerobic Oxidation of 5-Hydroxymethylfurfural into 2,5-Furandicarboxylic Acid in Water. *Catal. Sci. Technol.* **2015**, *5*, 3194–3202. [[CrossRef](#)]
144. Morales, G.; Melero, J.A.; Paniagua, M.; López-Aguado, C.; Vidal, N. Beta Zeolite as an Efficient Catalyst for the Synthesis of Diphenolic Acid (DPA) from Renewable Levulinic Acid. *Catal. Today*, 2022; *in press*. [[CrossRef](#)]
145. Obregón, I.; Gandarias, I.; Miletic, N.; Ocio, A.; Arias, P.L. One-Pot 2-Methyltetrahydrofuran Production from Levulinic Acid in Green Solvents Using Ni-Cu/Al₂O₃ Catalysts. *ChemSusChem* **2015**, *8*, 3483–3488. [[CrossRef](#)]
146. Muñoz-Olasagasti, M.; Sañudo-Mena, A.; Cecilia, J.A.; Granados, M.L.; Maireles-Torres, P.; Mariscal, R. Direct Conversion of Levulinic Acid into Valeric Biofuels Using Pd Supported Over Zeolites as Catalysts. *Top. Catal.* **2019**, *62*, 579–588. [[CrossRef](#)]
147. Shao, Y.; Sun, K.; Li, Q.; Liu, Q.; Zhang, S.; Liu, Q.; Hu, G.; Hu, X. Copper-Based Catalysts with Tunable Acidic and Basic Sites for the Selective Conversion of Levulinic Acid/Ester to γ -Valerolactone or 1,4-Pentanediol. *Green Chem.* **2019**, *21*, 4499–4511. [[CrossRef](#)]
148. Choudhary, H.; Nishimura, S.; Ebitani, K. Metal-Free Oxidative Synthesis of Succinic Acid from Biomass-Derived Furan Compounds Using a Solid Acid Catalyst with Hydrogen Peroxide. *Appl. Catal. A Gen.* **2013**, *458*, 55–62. [[CrossRef](#)]
149. Jiménez-Gómez, C.P.; Cecilia, J.A.; García-Sancho, C.; Moreno-Tost, R.; Maireles-Torres, P. Selective Production of Furan from Gas-Phase Furfural Decarbonylation on Ni-MgO Catalysts. *ACS Sustain. Chem. Eng.* **2019**, *7*, 7676–7685. [[CrossRef](#)]
150. Gupta, N.K.; Fukuoka, A.; Nakajima, K. Metal-Free and Selective Oxidation of Furfural to Furoic Acid with an N-Heterocyclic Carbene Catalyst. *ACS Sustain. Chem. Eng.* **2018**, *6*, 3434–3442. [[CrossRef](#)]
151. Lange, J.P.; Wadman, S.H. Furfural to 1,4-Butanediol/Tetrahydrofuran—A Detailed Catalyst and Process Design. *ChemSusChem* **2020**, *13*, 5329–5337. [[CrossRef](#)] [[PubMed](#)]
152. Gould, N.S.; Landfield, H.; Dinkelacker, B.; Brady, C.; Yang, X.; Xu, B. Selectivity Control in Catalytic Reductive Amination of Furfural to Furfurylamine on Supported Catalysts. *ChemCatChem* **2020**, *12*, 2106–2115. [[CrossRef](#)]
153. Tang, C.; Zhai, Z.; Li, X.; Sun, L.; Bai, W. Sustainable Production of Acetaldehyde from Lactic Acid over the Magnesium Aluminate Spinel. *J. Taiwan Inst. Chem. Eng.* **2016**, *58*, 97–106. [[CrossRef](#)]
154. Zhang, X.; Lin, L.; Zhang, T.; Liu, H.; Zhang, X. Catalytic Dehydration of Lactic Acid to Acrylic Acid over Modified ZSM-5 Catalysts. *Chem. Eng. J.* **2016**, *284*, 934–941. [[CrossRef](#)]
155. Zhang, C.; Wang, T.; Ding, Y. Oxidative Dehydrogenation of Lactic Acid to Pyruvic Acid over Pb-Pt Bimetallic Supported on Carbon Materials. *Appl. Catal. A Gen.* **2017**, *533*, 59–65. [[CrossRef](#)]
156. Chafran, L.S.; Campos, J.M.C.; Santos, J.S.; Sales, M.J.A.; Dias, S.C.L.; Dias, J.A. Synthesis of Poly(Lactic Acid) by Heterogeneous Acid Catalysis from d,l-Lactic Acid. *J. Polym. Res.* **2016**, *23*, 107. [[CrossRef](#)]
157. Li, X.; Sun, L.; Zou, W.; Cao, P.; Chen, Z.; Tang, C.; Dong, L. Efficient Conversion of Bio-Lactic Acid to 2,3-Pentanedione on Cesium-Doped Hydroxyapatite Catalysts with Balanced Acid–Base Sites. *ChemCatChem* **2017**, *9*, 4621–4627. [[CrossRef](#)]
158. Padula, I.D.; Santos, B.M.A.; Rodrigues, A.P.H.; Gasteloirs, P.L.; Mendes, I.M.C.; Portilho, M.F.; Oliveira, L.C.A.; Oliveira, C.C. Niobium-Modified Hydrotalcite Catalysts: Sustainable Conversion of Waste Glycerol to Valuable Chemicals. *Appl. Catal. A Gen.* **2020**, *606*, 117814. [[CrossRef](#)]
159. Shokrollahi Yancheshmeh, M.; Alizadeh Sahraei, O.; Aissaoui, M.; Iliuta, M.C. A Novel Synthesis of NiAl₂O₄ Spinel from a Ni-Al Mixed-Metal Alkoxide as a Highly Efficient Catalyst for Hydrogen Production by Glycerol Steam Reforming. *Appl. Catal. B* **2020**, *265*, 118535. [[CrossRef](#)]
160. Ali, B.; Lan, X.; Arslan, M.T.; Wang, H.; Gilani, S.Z.A.; Wang, S.; Wang, T. Self-Pillared MFI-Type Zeolite Nanosheets as Selective Catalysts for Glycerol Dehydration to Acrolein. *ACS Appl. Nano Mater.* **2020**, *3*, 10966–10977. [[CrossRef](#)]
161. Walgode, P.M.; Coelho, L.C.D.; Faria, R.P.V.; Rodrigues, A.E. Dihydroxyacetone Production: From Glycerol Catalytic Oxidation with Commercial Catalysts to Chromatographic Separation. *Ind. Eng. Chem. Res.* **2021**, *60*, 10551–10565. [[CrossRef](#)]
162. Ruiz, C.P.T.; Dumeignil, F.; Capron, M. Catalytic Production of Glycolic Acid from Glycerol Oxidation: An Optimization Using Response Surface Methodology. *Catalysts* **2021**, *11*, 257. [[CrossRef](#)]
163. Rossino, G.; Robescu, M.S.; Licastro, E.; Tedesco, C.; Martello, I.; Maffei, L.; Vincenti, G.; Bavaro, T.; Collina, S. Biocatalysis: A Smart and Green Tool for the Preparation of Chiral Drugs. *Chirality* **2022**, *34*, 1403–1418. [[CrossRef](#)]
164. Pollard, D.J.; Woodley, J.M. Biocatalysis for Pharmaceutical Intermediates: The Future Is Now. *Trends Biotechnol.* **2007**, *25*, 66–73. [[CrossRef](#)]
165. Sheldon, R.A. Biocatalysis, Solvents, and Green Metrics in Sustainable Chemistry. In *Biocatalysis in Green Solvents*; Academic Press: Cambridge, MA, USA, 2022.

166. Han, C.; Savage, S.; Al-Sayah, M.; Yajima, H.; Remarchuk, T.; Reents, R.; Wirz, B.; Iding, H.; Bachmann, S.; Fantasia, S.M.; et al. Asymmetric Synthesis of Akt Kinase Inhibitor Ipatasertib. *Org. Lett.* **2017**, *19*, 4806–4809. [\[CrossRef\]](#)
167. Patel, R.N. Biocatalysis: Synthesis of Key Intermediates for Development of Pharmaceuticals. *ACS Catal.* **2011**, *1*, 1056–1074. [\[CrossRef\]](#)
168. Wu, S.; Snajdrova, R.; Moore, J.C.; Baldenius, K.; Bornscheuer, U.T. Biocatalysis: Enzymatic Synthesis for Industrial Applications. *Angew. Chem.-Int. Ed.* **2021**, *60*, 88–119. [\[CrossRef\]](#) [\[PubMed\]](#)
169. St-Jean, F.; Angelaud, R.; Bachmann, S.; Carrera, D.E.; Remarchuk, T.; Piechowicz, K.A.; Niedermann, K.; Iding, H.; Meier, R.; Hou, H.; et al. Stereoselective Synthesis of the IDO Inhibitor Navoximod. *J. Org. Chem.* **2022**, *87*, 4955–4960. [\[CrossRef\]](#) [\[PubMed\]](#)
170. Molinaro, C.; Phillips, E.M.; Xiang, B.; Milczek, E.; Shevlin, M.; Balsells, J.; Ceglia, S.; Chen, J.; Chen, L.; Chen, Q.; et al. Synthesis of a CGRP Receptor Antagonist via an Asymmetric Synthesis of 3-Fluoro-4-Aminopiperidine. *J. Org. Chem.* **2019**, *84*, 8006–8018. [\[CrossRef\]](#) [\[PubMed\]](#)
171. Burns, M.; Martinez, C.A.; Vanderplas, B.; Wisdom, R.; Yu, S.; Singer, R.A. A Chemoenzymatic Route to Chiral Intermediates Used in the Multikilogram Synthesis of a Gamma Secretase Inhibitor. *Org. Process Res. Dev.* **2017**, *21*, 871–877. [\[CrossRef\]](#)
172. Novick, S.J.; Dellas, N.; Garcia, R.; Ching, C.; Bautista, A.; Homan, D.; Alvizo, O.; Entwistle, D.; Kleinbeck, F.; Schlama, T.; et al. Engineering an Amine Transaminase for the Efficient Production of a Chiral Sacubitril Precursor. *ACS Catal.* **2021**, *11*, 3762–3770. [\[CrossRef\]](#)
173. Schober, M.; MacDermaid, C.; Ollis, A.A.; Chang, S.; Khan, D.; Hosford, J.; Latham, J.; Ihnken, L.A.F.; Brown, M.J.B.; Fuerst, D.; et al. Chiral Synthesis of LSD1 Inhibitor GSK2879552 Enabled by Directed Evolution of an Imine Reductase. *Nat. Catal.* **2019**, *2*, 909–915. [\[CrossRef\]](#)
174. Connor, C.G.; Deforest, J.C.; Dietrich, P.; Do, N.M.; Doyle, K.M.; Eisenbeis, S.; Greenberg, E.; Griffin, S.H.; Jones, B.P.; Jones, K.N.; et al. Development of a Nitrene-Type Rearrangement for the Commercial Route of the JAK1 Inhibitor Abrocitinib. *Org. Process Res. Dev.* **2021**, *25*, 608–615. [\[CrossRef\]](#)
175. Galvão, W.S.; Pinheiro, B.B.; Golçalves, L.R.B.; de Mattos, M.C.; Fonseca, T.S.; Regis, T.; Zampieri, D.; dos Santos, J.C.S.; Costa, L.S.; Correa, M.A.; et al. Novel Nanohybrid Biocatalyst: Application in the Kinetic Resolution of Secondary Alcohols. *J. Mater. Sci.* **2018**, *53*, 14121–14137. [\[CrossRef\]](#)
176. Tang, C.D.; Ding, P.J.; Shi, H.L.; Jia, Y.Y.; Zhou, M.Z.; Yu, H.L.; Xu, J.H.; Yao, L.G.; Kan, Y.C. One-Pot Synthesis of Phenylglyoxylic Acid from Racemic Mandelic Acids via Cascade Biocatalysis. *J. Agric. Food Chem.* **2019**, *67*, 2946–2953. [\[CrossRef\]](#)
177. Han, S.W.; Park, E.S.; Dong, J.Y.; Shin, J.S. Mechanism-Guided Engineering of ω -Transaminase to Accelerate Reductive Amination of Ketones. *Adv. Synth. Catal.* **2015**, *357*, 1732–1740. [\[CrossRef\]](#)
178. Wang, H.; Fan, H.; Sun, H.; Zhao, L.; Wei, D. Process Development for the Production of (R)-(-)-Mandelic Acid by Recombinant Escherichia Coli Cells Harboring Nitrilase from *Burkholderia cenocepacia* J2315. *Org. Process Res. Dev.* **2015**, *19*, 2012–2016. [\[CrossRef\]](#)
179. Schmölder, K.; Weingarten, M.; Baldenius, K.; Nidetzky, B. Glycosynthase Principle Transformed into Biocatalytic Process Technology: Lacto- N-Triose II Production with Engineered Exo-Hexosaminidase. *ACS Catal.* **2019**, *9*, 5503–5514. [\[CrossRef\]](#)
180. Wohlgemuth, R. The Power of Biocatalysts for Highly Selective and Efficient Phosphorylation Reactions. *Catalysts* **2022**, *12*, 1436. [\[CrossRef\]](#)
181. Tamboli, A.H.; Chaugule, A.A.; Gosavi, S.W.; Kim, H. $Ce_xZr_{1-x}O_2$ Solid Solutions for Catalytic Synthesis of Dimethyl Carbonate from CO_2 : Reaction Mechanism and the Effect of Catalyst Morphology on Catalytic Activity. *Fuel* **2018**, *216*, 245–254. [\[CrossRef\]](#)
182. Luis, P. Use of Monoethanolamine (MEA) for CO_2 Capture in a Global Scenario: Consequences and Alternatives. *Desalination* **2016**, *380*, 93–99. [\[CrossRef\]](#)
183. Chen, Y.; Mu, T. Conversion of CO_2 to Value-Added Products Mediated by Ionic Liquids. *Green Chem.* **2019**, *21*, 2544–2574. [\[CrossRef\]](#)
184. Zhao, Y.; Liu, Z. Transformation of CO_2 into Valuable Chemicals. In *Encyclopedia of Sustainability Science and Technology*; Springer: Berlin/Heidelberg, Germany, 2018.
185. Ateka, A.; Rodriguez-Vega, P.; Ereña, J.; Aguayo, A.T.; Bilbao, J. A Review on the Valorization of CO_2 . Focusing on the Thermodynamics and Catalyst Design Studies of the Direct Synthesis of Dimethyl Ether. *Fuel Process. Technol.* **2022**, *233*, 107310. [\[CrossRef\]](#)
186. Lee, J.H.; Lee, J.H.; Park, I.K.; Lee, C.H. Techno-Economic and Environmental Evaluation of CO_2 Mineralization Technology Based on Bench-Scale Experiments. *J. CO_2 Util.* **2018**, *26*, 522–536. [\[CrossRef\]](#)
187. Gao, D.; Li, W.; Wang, H.; Wang, G.; Cai, R. Heterogeneous Catalysis for CO_2 Conversion into Chemicals and Fuels. *Trans. Tianjin Univ.* **2022**, *28*, 245–264. [\[CrossRef\]](#)
188. Fegade, U.; Jethave, G. Conversion of Carbon Dioxide into Formic Acid. In *Conversion of Carbon Dioxide into Hydrocarbons Vol. 2 Technology*; Springer: Cham, Switzerland, 2020; pp. 91–110. [\[CrossRef\]](#)
189. Chen, Y.; Wang, H.; Qin, Z.; Tian, S.; Ye, Z.; Ye, L.; Abroshan, H.; Li, G. $Ti_xCe_{1-x}O_2$ Nanocomposites: A Monolithic Catalyst for the Direct Conversion of Carbon Dioxide and Methanol to Dimethyl Carbonate. *Green Chem.* **2019**, *21*, 4642–4649. [\[CrossRef\]](#)
190. Kongpanna, P.; Pavarajarn, V.; Gani, R.; Assabumrungrat, S. Techno-Economic Evaluation of Different CO_2 -Based Processes for Dimethyl Carbonate Production. *Chem. Eng. Res. Des.* **2015**, *93*, 496–510. [\[CrossRef\]](#)

191. Ohno, H.; Ikhlaiel, M.; Tamura, M.; Nakao, K.; Suzuki, K.; Morita, K.; Kato, Y.; Tomishige, K.; Fukushima, Y. Direct Dimethyl Carbonate Synthesis from CO₂ and Methanol Catalyzed by CeO₂ and Assisted by 2-Cyanopyridine: A Cradle-to-Gate Greenhouse Gas Emission Study. *Green Chem.* **2021**, *23*, 457–469. [[CrossRef](#)]
192. Honda, M.; Tamura, M.; Nakagawa, Y.; Nakao, K.; Suzuki, K.; Tomishige, K. Organic Carbonate Synthesis from CO₂ and Alcohol over CeO₂ with 2-Cyanopyridine: Scope and Mechanistic Studies. *J. Catal.* **2014**, *318*, 95–107. [[CrossRef](#)]
193. Tomishige, K.; Tamura, M.; Nakagawa, Y. CO₂ Conversion with Alcohols and Amines into Carbonates, Ureas, and Carbamates over CeO₂ Catalyst in the Presence and Absence of 2-Cyanopyridine. *Chem. Rec.* **2019**, *19*, 1354–1379. [[CrossRef](#)]
194. Gonçalves, R.V.; Vono, L.L.R.; Wojcieszak, R.; Dias, C.S.B.; Wender, H.; Teixeira-Neto, E.; Rossi, L.M. Selective Hydrogenation of CO₂ into CO on a Highly Dispersed Nickel Catalyst Obtained by Magnetron Sputtering Deposition: A Step towards Liquid Fuels. *Appl. Catal. B* **2017**, *209*, 240–246. [[CrossRef](#)]
195. Vural Gürsel, I.; Noël, T.; Wang, Q.; Hessel, V. Separation/Recycling Methods for Homogeneous Transition Metal Catalysts in Continuous Flow. *Green Chem.* **2015**, *17*, 2012–2026. [[CrossRef](#)]
196. Miceli, M.; Frontera, P.; Macario, A.; Malara, A. Recovery/Reuse of Heterogeneous Supported Spent Catalysts. *Catalysts* **2021**, *11*, 591. [[CrossRef](#)]
197. Shende, V.S.; Saptal, V.B.; Bhanage, B.M. Recent Advances Utilized in the Recycling of Homogeneous Catalysis. *Chem. Rec.* **2019**, *19*, 2022–2043. [[CrossRef](#)]
198. Santoro, S.; Kozhushkov, S.I.; Ackermann, L.; Vaccaro, L. Heterogeneous Catalytic Approaches in C-H Activation Reactions. *Green Chem.* **2016**, *18*, 3471–3493. [[CrossRef](#)]
199. Sádaba, I.; López Granados, M.; Riisager, A.; Taarning, E. Deactivation of Solid Catalysts in Liquid Media: The Case of Leaching of Active Sites in Biomass Conversion Reactions. *Green Chem.* **2015**, *17*, 4133–4145. [[CrossRef](#)]
200. Chiranjeevi, T.; Pragya, R.; Gupta, S.; Gokak, D.T.; Bhargava, S. Minimization of Waste Spent Catalyst in Refineries. *Procedia Environ. Sci.* **2016**, *35*, 610–617. [[CrossRef](#)]
201. Liu, X.-H.; Ma, J.-G.; Niu, Z.; Yang, G.-M.; Cheng, P. An Efficient Nanoscale Heterogeneous Catalyst for the Capture and Conversion of Carbon Dioxide at Ambient Pressure. *Angew. Chem.* **2015**, *127*, 1002–1005. [[CrossRef](#)]
202. Martinson, K.D.; Kondrashkova, I.S.; Omarov, S.O.; Sladkovskiy, D.A.; Kiselev, A.S.; Kiseleva, T.Y.; Popkov, V.I. Magnetically Recoverable Catalyst Based on Porous Nanocrystalline HoFeO₃ for Processes of N-Hexane Conversion. *Adv. Powder Technol.* **2020**, *31*, 402–408. [[CrossRef](#)]
203. Hu, J.; Wang, X.; Xiao, L.; Song, S.; Zhang, B. Removal of Vanadium from Molybdate Solution by Ion Exchange. *Hydrometallurgy* **2009**, *95*, 203–206. [[CrossRef](#)]
204. Peng, Z.; Li, Z.; Lin, X.; Tang, H.; Ye, L.; Ma, Y.; Rao, M.; Zhang, Y.; Li, G.; Jiang, T. Pyrometallurgical Recovery of Platinum Group Metals from Spent Catalysts. *JOM* **2017**, *69*, 1553–1562. [[CrossRef](#)]
205. Wang, J.; Zhou, C.C.; Gao, Z.; Feng, X.; Yamamoto, Y.; Bao, M. Unsupported Nanoporous Palladium Catalyst for Highly Selective Hydrogenation of Carbon Dioxide and Sodium Bicarbonate into Formate. *ChemCatChem* **2021**, *13*, 2702–2708. [[CrossRef](#)]
206. Zhu, F.; Zhu-Ge, L.; Yang, G.; Zhou, S. Iron-Catalyzed Hydrogenation of Bicarbonates and Carbon Dioxide to Formates. *ChemSusChem* **2015**, *8*, 609–612. [[CrossRef](#)]
207. Sengupta, S.; Jha, A.; Shende, P.; Maskara, R.; Das, A.K. Catalytic Performance of Co and Ni Doped Fe-Based Catalysts for the Hydrogenation of CO₂ to CO via Reverse Water-Gas Shift Reaction. *J. Environ. Chem. Eng.* **2019**, *7*, 102911. [[CrossRef](#)]
208. Dong, X.; Li, F.; Zhao, N.; Tan, Y.; Wang, J.; Xiao, F. CO₂ Hydrogenation to Methanol over Cu/Zn/Al/Zr Catalysts Prepared by Liquid Reduction. *Cuihua Xuebao/Chin. J. Catal.* **2017**, *38*, 717–725. [[CrossRef](#)]
209. Gao, P.; Yang, H.; Zhang, L.; Zhang, C.; Zhong, L.; Wang, H.; Wei, W.; Sun, Y. Fluorinated Cu/Zn/Al/Zr Hydrotalcites Derived Nanocatalysts for CO₂ Hydrogenation to Methanol. *J. CO₂ Util.* **2016**, *16*, 32–41. [[CrossRef](#)]
210. Lee, T.; Jung, S.; Baek, K.; Tsang, Y.F.; Lin, K.Y.A.; Jeon, Y.J.; Kwon, E.E. Functional Use of CO₂ to Mitigate the Formation of Bisphenol A in Catalytic Pyrolysis of Polycarbonate. *J. Hazard. Mater.* **2022**, *423*, 126992. [[CrossRef](#)] [[PubMed](#)]
211. Haque, N.; Biswas, S.; Ghosh, S.; Chowdhury, A.H.; Khan, A.; Islam, S.M. Zn(II)-Embedded Nanoporous Covalent Organic Frameworks for Catalytic Conversion of CO₂ under Solvent-Free Conditions. *ACS Appl. Nano Mater.* **2021**, *4*, 7663–7674. [[CrossRef](#)]
212. Fan, G.; Luo, S.; Wu, Q.; Fang, T.; Li, J.; Song, G. ZnBr₂ Supported on Silica-Coated Magnetic Nanoparticles of Fe₃O₄ for Conversion of CO₂ to Diphenyl Carbonate. *RSC Adv.* **2015**, *5*, 56478–56485. [[CrossRef](#)]
213. Qian, Q.; Zhang, J.; Cui, M.; Han, B. Synthesis of Acetic Acid via Methanol Hydrocarboxylation with CO₂ and H₂. *Nat. Commun.* **2016**, *7*, 11481. [[CrossRef](#)]
214. Lee, J.; Kim, K.H.; Kwon, E.E. Biochar as a Catalyst. *Renew. Sustain. Energy Rev.* **2017**, *77*, 70–79. [[CrossRef](#)]
215. Tong, S.; Zhang, S.; Yin, H.; Wang, J.; Chen, M. Study on Co-Hydrothermal Treatment Combined with Pyrolysis of Rice Straw/Sewage Sludge: Biochar Properties and Heavy Metals Behavior. *J. Anal. Appl. Pyrolysis* **2021**, *155*, 105074. [[CrossRef](#)]
216. Cheng, F.; Li, X. Preparation and Application of Biochar-Based Catalysts for Biofuel Production. *Catalysts* **2018**, *8*, 346. [[CrossRef](#)]
217. Ormsby, R.; Kastner, J.R.; Miller, J. Hemicellulose Hydrolysis Using Solid Acid Catalysts Generated from Biochar. *Catal. Today* **2012**, *190*, 89–97. [[CrossRef](#)]
218. Xiong, X.; Yu, I.K.M.; Chen, S.S.; Tsang, D.C.W.; Cao, L.; Song, H.; Kwon, E.E.; Ok, Y.S.; Zhang, S.; Poon, C.S. Sulfonated Biochar as Acid Catalyst for Sugar Hydrolysis and Dehydration. *Catal. Today* **2018**, *314*, 52–61. [[CrossRef](#)]

219. Paulinetti, A.P.; Augusto, I.M.G.; Batista, L.P.P.; Tavares, A.G.B.; Albanez, R.; Ratusznei, S.M.; Lovato, G.; Rodrigues, J.A.D. Anaerobic Digestion as a Core Process for Sustainable Energy Production in the Soybean Biorefinery: A Techno-economic Assessment. *Sustain. Horiz.* **2022**, *3*, 100024. [[CrossRef](#)]
220. Loy, A.C.M.; Alhazmi, H.; Lock, S.S.M.; Yiin, C.L.; Cheah, K.W.; Chin, B.L.F.; How, B.S.; Yusup, S. Life-Cycle Assessment of Hydrogen Production via Catalytic Gasification of Wheat Straw in the Presence of Straw Derived Biochar Catalyst. *Bioresour. Technol.* **2021**, *341*, 125796. [[CrossRef](#)]
221. Kim, H.; Choi, J.; Park, J.; Won, W. Production of a Sustainable and Renewable Biomass-Derived Monomer: Conceptual Process Design and Techno-Economic Analysis. *Green Chem.* **2020**, *22*, 7070–7079. [[CrossRef](#)]
222. Carmona-Garcia, E.; Mann-Valencia, P.A.; Solarte-Toro, J.C.; Moustakas, K.; Cardona-Alzate, C.A. Comparison of Acetone-Butanol-Ethanol Fermentation and Ethanol Catalytic Upgrading as Pathways for Butanol Production: A Techno-Economic and Environmental Assessment. *Biofuel Res. J.* **2021**, *8*, 1384. [[CrossRef](#)]
223. Solarte-Toro, J.C.; Romero-García, J.M.; Martínez-Patiño, J.C.; Ruiz-Ramos, E.; Castro-Galiano, E.; Cardona-Alzate, C.A. Acid Pretreatment of Lignocellulosic Biomass for Energy Vectors Production: A Review Focused on Operational Conditions and Techno-Economic Assessment for Bioethanol Production. *Renew. Sustain. Energy Rev.* **2019**, *107*, 587–601. [[CrossRef](#)]

Disclaimer/Publisher’s Note: The statements, opinions and data contained in all publications are solely those of the individual author(s) and contributor(s) and not of MDPI and/or the editor(s). MDPI and/or the editor(s) disclaim responsibility for any injury to people or property resulting from any ideas, methods, instructions or products referred to in the content.